AEDC-TR-59-3
ASTIA DOCUMENT NO.:
AD-208774

Copy 1

A METHOD OF CALCULATING TURBULENT-BOUNDARY-LAYER GROWTH AT HYPERSONIC MACH NUMBERS

By
James C. Sivells and Robert G. Payne
GDF, ARO, Inc.

March 1959

ARNOLD ENGINEERING DEVELOPMENT CENTER
AIR RESEARCH AND DEVELOPMENT COMMAND
USAF

AEDC-TR-59-3
ASTIA DOCUMENT NO.:
AD-208774

A METHOD OF CALCULATING TURBULENT-BOUNDARY-LAYER GROWTH AT HYPERSONIC MACH NUMBERS

By
James C. Sivells and Robert G. Payne
GDF, ARO, Inc.

March 1959

ARO Project No. 347802

Contract No. AF 40(600)-700 S/A 13(59-1)

CONTENTS

TABLE

ILLUSTRATIONS

ABSTRACT

A method is developed for calculating the growth of a turbulent boundary layer at hypersonic Mach numbers. Excellent agreement with experimental results from axisymmetric nozzles has been obtained by the application of this method. The method utilizes a modification of Stewartson's transformation to simplify the integration of the momentum equation. Heat transfer is taken into account by evaluating the gas properties at Eckert's reference temperature and by using a modification of Crocco's quadratic for the temperature distribution in the boundary layer. A new empirical relation is used for the incompressible friction coefficient which agrees with experimental data over a Reynolds number range from 10^5 to 10^9.

NOMENCLATURE

A	Flow area
a	Speed of sound
C_f	Local skin-friction coefficient
C_F	Mean skin-friction coefficient
h	Enthalpy
H	Boundary layer form factor
M	Mach number
N	Parameter in power-law equations for skin friction
P	Function defined in Eq. (4)
p	Pressure
Q	Function defined in Eq. (4)
R*	Radius of curvature of nozzle at the throat
R_x	Reynolds number based on x
R_X	Incompressible Reynolds number based on X
$R\theta$	Reynolds number based on θ
r	Local distance from axis of flow to wall
s	Distance measured along wall surface
T	Temperature
U	Transformed velocity component parallel to wall

u	Velocity component parallel to wall
X	Transformed coordinate along axis of flow
x	Coordinate along axis of flow
Y	Transformed coordinate normal to wall
y	Coordinate normal to wall
α	Function defined in Eq. (20)
β	Function defined in Eq. (21)
γ	Ratio of specific heats
δ^*	Boundary-layer displacement thickness
Δ	Boundary-layer thickness
θ	Boundary-layer momentum thickness
μ	Dynamic viscosity
ρ	Density
τ_w	Shearing stress at wall
ω	Angle of wall surface with respect to axis

Subscripts

aw	Value at adiabatic wall conditions
e	Value at free-stream static conditions
i	Value for incompressible flow
o	Value at free-stream stagnation conditions
s	Local stagnation temperature
t	Total
tr	Transformed
w	Evaluated at the wall

Superscripts

$*$	Evaluated at $M = 1$ except δ^*
$'$	Evaluated at reference temperature

INTRODUCTION

Many investigators have studied the problem of calculating the growth of turbulent boundary layers. For the incompressible adiabatic case, such calculations are fairly straightforward since they depend only upon the empirical relationship of the skin-friction coefficient with Reynolds number when the pressure gradients in the direction of flow are favorable or absent (Ref. 1). Even in the presence of adverse pressure gradients, empirical methods have been devised for the purpose of predicting the location of separation (Ref. 2).

As the speed of the gas outside the boundary layer increases, the effects of compressibility on the skin-friction coefficient must also be taken into account. For many cases in supersonic flow, the heat transfer between the gas and the wall may be neglected and methods such as Tucker's (Ref. 3) may be used to calculate the boundary-layer growth. There is enough difference, however, between the free-stream static temperature and the adiabatic wall temperature that some intermediate "reference" temperature must be used for evaluating the compressible skin-friction coefficient in order to obtain good correlation with experimental results. Tucker uses a reference temperature equal to the arithmetic average of the adiabatic wall temperature and the free-stream static temperature.

For gases with a Prandtl number of 1, the adiabatic wall temperature is equal to the stagnation temperature and the thermal boundary layer has the same thickness as the velocity boundary layer. For gases such as air which have a Prandtl number less than 1, the adiabatic wall temperature is less than the stagnation temperature and the thermal boundary layer is thicker than the velocity boundary layer. Bartz (Ref. 4) attempts to take this effect into account, together with the effect of heat transfer, by obtaining simultaneous solutions of the momentum equation and the energy equation. He, however, restricts his solution to a one-seventh-power velocity profile and uses a reference temperature equal to the arithmetic average of the wall temperature and free-stream static temperature.

When the wall temperature is much lower than the adiabatic wall temperature (often the situation at hypersonic speeds), the reference temperature should be somewhat higher than the arithmetic mean between the wall and free-stream static temperature as shown by Sommer and Short (Ref. 5) and Tendeland (Ref. 6). The reference temperature suggested by Eckert (Ref. 7) correlates with existing data as well as that used by Sommer and Short. Persh (Ref. 8)

Manuscript released by authors January 1959.

attempts to account for this same effect by using a reference temperature equal to the temperature at the edge of the laminar sub-layer, where this temperature is defined as a function of velocity ratio according to Crocco's quadratic modified by using the adiabatic wall temperature to account for the Prandtl number being less than one.

One important use of an accurate method of calculating turbulent-boundary-layer growth at hypersonic Mach numbers is in the design of axisymmetric hypersonic wind tunnels. The perfect-fluid (potential-flow) contour can be accurately calculated by the method of characteristics, but the attainment of uniform flow in the test region depends also upon the accuracy of the boundary-layer correction to the theoretical contour. Each of the available methods of calculating boundary-layer growth possessed some drawback. This fact led to the development of the method described herein, which utilizes a modification of Stewartson's transformation (Ref. 9) to aid in the integration of the momentum equation. The main difference, however, between this method and other methods is in the evaluation of the compressible skin-friction coefficient and the transformed form factor. In order to simplify the calculations, a new empirical equation was developed for the incompressible skin-friction coefficient which agrees with experimental data over a range of Reynolds number (R_{x_i}) from 10^5 to 10^9. Excellent correlations have been obtained between experimental values of boundary-layer displacement thickness and those calculated by this method.

Since this method was developed primarily for hypersonic wind tunnels, it may not be suitable where adverse pressure gradients are present or where the temperatures are sufficiently high to cause dissociation.

DEVELOPMENT OF METHOD

MOMENTUM EQUATION

For the purpose of this report, steady compressible flow is assumed. Thus, the von Karman momentum equation for axisymmetric flow can be written in the form:

$$\frac{d\theta}{ds} + \theta \left[\frac{2 - M^2 + H}{M\left(1 + \frac{\gamma - 1}{2} M^2\right)} \frac{dM}{ds} + \frac{1}{r} \frac{dr}{ds} \right] = \frac{C_f}{2} \tag{1}$$

In order to obtain a solution for the momentum thickness θ, the values of M, H, r, and C_f must be known as a function of distance s along the surface. For many cases, such as wind tunnel nozzles, these values are known as a function of distance x along the center line. Since

$$\frac{ds}{dx} = \sqrt{1 + \left(\frac{dr}{dx}\right)^2} = \sec \omega \tag{2}$$

Eq. (1) may be written as

$$\frac{d\theta}{dx} + \theta \left[\frac{2 - M^2 + H}{M\left(1 + \frac{\gamma - 1}{2} M^2\right)} \frac{dM}{dx} + \frac{1}{r} \frac{dr}{dx} \right] = \frac{C_f}{2} \sec \omega \tag{3}$$

When ω is small, the assumption that sec ω = 1 can be made with negligible consequences.

It can be recognized that Eq. (3) is a linear, first-order, ordinary differential equation of the form

$$\frac{d\theta}{dx} + \theta P(x) = Q(x) \tag{4}$$

which has the solution

$$\theta(x) = e^{-\int P dx} \left[\int Q(x)\, e^{\int P dx}\, dx + \text{constant} \right] \tag{5}$$

Since P(x) and Q(x) are generally non-analytic functions of x, numerical methods must be used to evaluate the indicated integrations.

The solution of Eq. (3) is considerably simplified, however, through the use of the equations

$$\theta = \theta_{tr} \left(1 + \frac{\gamma - 1}{2} M^2\right)^{\frac{\gamma + 1}{2(\gamma - 1)}} = \theta_{tr} \left(\frac{T_o}{T_e}\right)^{\frac{\gamma + 1}{2(\gamma - 1)}} \tag{6}$$

and

$$H = H_{tr}\left(1 + \frac{\gamma - 1}{2} M^2\right) + \frac{\gamma - 1}{2} M^2 \tag{7a}$$

or

$$H + 1 = (H_{tr} + 1) \frac{T_o}{T_e} \tag{7b}$$

which are obtained from Stewartson's transformation as shown in Appendix A. By substituting Eq. (6) and (7) into Eq. (3), the equation

$$\frac{d\theta_{tr}}{dx} + \frac{\theta_{tr}}{M} \frac{dM}{dx} (2 + H_{tr}) + \frac{\theta_{tr}}{r} \frac{dr}{dx} = \frac{C_f}{2} \sec \omega \left(\frac{T_e}{T_o}\right)^{\frac{\gamma + 1}{2(\gamma - 1)}} \tag{8}$$

is obtained. By multiplying Eq. (8) by $r M^{2 + H_{tr}}$, the left-hand side becomes a perfect differential if H_{tr} is assumed to be constant over the interval of integration. Therefore,

$$\left(\theta_{tr}\, r\, M^{2 + H_{tr}}\right)_b - \left(\theta_{tr}\, r\, M^{2 + H_{tr}}\right)_a = \int_a^b r\, M^{2 + H_{tr}} \sec \omega \, \frac{C_f}{2} \left(\frac{T_e}{T_o}\right)^{\frac{\gamma + 1}{2(\gamma - 1)}} dx \qquad (9)$$

Thus, the solution of the momentum equation is reduced to a single integration which, in general, must be accomplished by numerical methods.

Substitution of Eq. (6) into Eq. (9) yields

$$\left[\theta\, r M^{2 + H_{tr}} \left(\frac{T_e}{T_o}\right)^{\frac{\gamma + 1}{2(\gamma - 1)}}\right]_b - \left[\theta\, r M^{2 + H_{tr}} \left(\frac{T_e}{T_o}\right)^{\frac{\gamma + 1}{2(\gamma - 1)}}\right]_a = \int_a^b r M^{2 + H_{tr}} \sec \omega \, \frac{C_f}{2} \left(\frac{T_e}{T_o}\right)^{\frac{\gamma + 1}{2(\gamma - 1)}} dx \qquad (10)$$

It may be noted that, as long as H_{tr} as defined by Eq. (7) is approximately constant, Eq. (6) and (7) may be considered to be merely integrating aids irrespective of the validity of Stewartson's transformation.

When there is no heat transfer and the Prandtl number is one, the transformed form factor becomes equal to the incompressible value. In an attempt to account for heat transfer and for Prandtl numbers other than one, use is made of Crocco's quadratic for the temperature distribution in the boundary layer according to the equation

$$\frac{T}{T_e} = \frac{T_w}{T_e} - \left(\frac{T_w - T_{aw}}{T_e}\right)\left(\frac{u}{u_e}\right) - \left(\frac{T_{aw} - T_e}{T_e}\right)\left(\frac{u}{u_e}\right)^2 \qquad (11)$$

which is the form used by Persh (Ref. 8). As shown in Appendix A, the use of this equation yields

$$H = H_i \left(\frac{T_w}{T_e}\right) + \left(\frac{T_{aw} - T_e}{T_e}\right) \qquad (12)$$

Combining Eqs. (7) and (12) gives

$$H_{tr} = H_i \frac{T_w}{T_o} + \frac{T_{aw}}{T_o} - 1 \qquad (13)$$

which relates the transformed form factor in terms of the incompressible value and the temperature ratios.

For the evaluation of Eq. (1) for a particular problem, values of r, M, ω, and γ are given as functions of x. With the wall temperature given or assumed as a function of x, H_{tr} may be found by Eq. (13) in terms of H_i. Still remaining to be determined are C_f and H_i, which are considered in subsequent sections.

DETERMINATION OF C_f

The compressible skin-friction coefficient C_f in Eq. (10) is a function of Mach number, Reynolds number, and heat transfer and is defined in terms of the shearing stress at the wall,

$$\frac{C_f}{2} = \frac{\tau_w}{\rho_e u_e^2} \tag{14}$$

In the evaluation of C_f, efforts are made to obtain empirical correlations with the incompressible value which is a function of Reynolds number based either on the momentum thickness or distance,

$$\frac{C_{f_i}}{2} = \frac{\tau_w}{\rho_o u_e^2} = F(R\theta_i) = G(R_{x_i}) \tag{15}$$

The assumption has been made that there is some reference point in the compressible boundary layer where the temperature and density are such that

$$\frac{C_f'}{2} = \frac{\tau_w}{\rho' u_e^2} = F(R\theta') = G(R_x') \tag{16}$$

where

$$R\theta' = \frac{\rho' u_e \theta}{\mu'} \tag{17}$$

$$R_x' = \frac{\rho' u_e x}{\mu'} \tag{18}$$

and the values of ρ' and μ' are evaluated at the reference temperature. Therefore,

$$\frac{C_f}{2} = \frac{\rho'}{\rho_e} \frac{C_f'}{2} = \frac{T_e}{T'} \frac{C_f'}{2} \tag{19}$$

since the pressure is assumed to be constant through the boundary layer.

It may be shown, however, that

$$\frac{T_e}{T'} F(R\theta') \neq \frac{T_e}{T'} G(R_x')$$

by using the power-law equations for skin-friction coefficient

$$F(R_{\theta}') = \frac{\alpha}{(R_{\theta}')^{\frac{1}{N}}} \tag{20}$$

and

$$G(R_x') = \frac{\beta}{(R_x')^{\frac{1}{N+1}}} \tag{21}$$

where

$$\beta = \frac{\alpha^{\frac{N}{N+1}}}{\left(\frac{N+1}{N}\right)^{\frac{1}{N+1}}} \tag{22}$$

can be derived from the incompressible relationships. In the absence of pressure gradient, Eq. (1) can be written as

$$\frac{d\theta}{dx} = \frac{C_f}{2} \tag{23}$$

If

$$\frac{C_f}{2} = \frac{T_e}{T'} F(R_{\theta}') = \frac{T_e}{T'} \frac{\alpha}{\left(\frac{\rho' u_e \theta}{u'}\right)^{\frac{1}{N}}} \tag{24}$$

then

$$\theta^{\frac{1}{N}} d\theta = \left(\frac{T_e}{T'}\right) \alpha \left(\frac{\mu'}{\rho' u_e}\right)^{\frac{1}{N}} dx \tag{25}$$

and, after integrating,

$$\frac{C_F}{2} = \frac{\theta}{x} = \left(\frac{T_e}{T'}\right)^{\frac{N}{N+1}} \frac{\left(\frac{N+1}{N} \alpha\right)^{\frac{N}{N+1}}}{(R_x')^{\frac{1}{N+1}}} \tag{26}$$

On the other hand, if

$$\frac{C_f}{2} = \frac{T_e}{T'} G(R_x') = \frac{T_e}{T'} \frac{\beta}{\left(\frac{\rho' u_e x}{\mu}\right)^{\frac{1}{N+1}}} \tag{27}$$

then

$$d\theta = \frac{T_e}{T'} \beta \left(\frac{\mu'}{\rho' u_e} \right)^{\frac{1}{N+1}} \frac{dx}{x^{\frac{1}{N+1}}} \tag{28}$$

and, after integrating,

$$\frac{C_F}{2} = \frac{\theta}{x} = \frac{T_e}{T'} \frac{\frac{N+1}{N} \beta}{(R_x')^{\frac{1}{N+1}}} = \frac{T_e}{T'} \frac{\left(\frac{N+1}{N} \alpha\right)^{\frac{N}{N+1}}}{(R_x')^{\frac{1}{N+1}}} \tag{29}$$

It is obvious that Eq. (26) is not equal to Eq. (29), and therefore Eq. (24) and Eq. (27) cannot both be correct. Experimental correlation must be made to determine which equation gives the better results.

The determination of the proper value of reference temperature to be used must also depend upon experimental correlation. Eckert (Ref. 7) suggests the relation

$$T' = 0.5\ T_w + 0.22\ T_{aw} + 0.28\ T_e \tag{30}$$

which, if the recovery factor is equal to 0.896, becomes

$$T' = 0.5\ T_w + (0.5 + 0.0394\ M^2)\ T_e \tag{31}$$

Sommer and Short (Ref. 5) suggest the relation

$$T' = 0.45\ T_w + (0.55 + 0.035\ M^2)\ T_e \tag{32}$$

which, again if the recovery factor is equal to 0.896, becomes

$$T' = 0.45\ T_w + 0.195\ T_{aw} + 0.355\ T_e \tag{33}$$

Eckert's relation shows slightly greater effects of both heat transfer and Mach number than does that of Sommer and Short and appears to give slightly better correlation with the meager amount of data which exists at hypersonic Mach numbers. In order to take into account the effects of variable specific heat, Eckert suggests the use of a reference enthalpy

$$h' = 0.5\ h_w + 0.22\ h_{aw} + 0.28\ h_e \tag{34}$$

for evaluating the physical properties of the gas. Although the derivations described herein are developed for constant specific heat, this modification can be easily substituted throughout.

The correlation of theoretical results with experimental data can be made by comparing the ratios of compressible skin-friction coefficients to the incompressible value at the same free-stream Reynolds number. Most of the experimental data have been obtained in wind tunnels. In the supersonic range up to a Mach number of about 5, stagnation temperatures are of the order of 100° F or 560° R while the static temperatures decrease with increasing Mach number until a value of about 100° R is reached. At higher Mach numbers, the stagnation temperature is increased to maintain the static temperature at about 100° R in order to avoid liquefaction of the constituents of the air. The temperature variation which is suggested for correlating wind tunnel results is shown in Fig. 1 along with Eckert's reference temperature for the adiabatic wall condition. The temperature range is so great that a simple power law for the variation of viscosity with temperature is not valid, and Sutherland's law must be used above 198.7° R. Below this temperature, there is some meager evidence that the viscosity varies proportionally with the temperature (the curve is tangent to the Sutherland curve). Misleading results can be obtained if such factors are not taken into account for correlation over a wide range in Mach numbers.

A correlation of C_f/C_{f_i} as a function of Mach number is shown in Fig. 2. The experimental data were taken from Refs. 10 through 17 and are for approximately adiabatic wall conditions. The values of C_{f_i} used for the ratios were obtained from the relation

$$C_{f_i} = \frac{0.088\ (\log R_{x_i} - 2.3686)}{(\log R_{x_i} - 1.5)^3} \tag{35}$$

which is developed in Appendix B. The values of C_f were obtained from the relation

$$C_f = \frac{T_e}{T'} \frac{0.088\ (\log R_x' - 2.3686)}{(\log R_x' - 1.5)^3} \tag{36}$$

where

$$R_x' = \frac{\rho' u_e x}{\mu'} = \frac{T_e \mu_e}{T' \mu'} R_x \tag{37}$$

and R_x, the free-stream Reynolds number, is the same as R_{x_i} for this curve. The static and reference temperatures from Fig. 1 were used to obtain the ratio of C_f/C_{f_i} shown in Fig. 2. The good correlation shown indicates that Eq. (36) provides an adequate method of determining C_f for use in Eq. (10). It should be noted that Eq. (36) is of the general form of Eq. (27) which therefore represents experimental results better than Eq. (24).

Much of the experimental data is available in terms of R_θ. The corresponding value of R_x can be found from Eq. (36) in the same manner in which Eq. (29) was obtained from Eq. (27).

$$\theta = \int_0^x \frac{T_e}{T'} \frac{0.044\ (\log R_x' - 2.3686)}{(\log R_x' - 1.5)^3}\, dx \tag{38}$$

After integration

$$\frac{C_F}{2} = \frac{\theta}{x} = \frac{R_\theta}{R_x} = \frac{T_e}{T'} \frac{0.044}{(\log R_x' - 1.5)^2} \tag{39}$$

Therefore

$$R_\theta = \frac{\mu'}{\mu_e} \frac{0.044\ R_x'}{(\log R_x' - 1.5)^2} \tag{40}$$

From this equation, the determination of R_θ is straightforward when R_x' is given; however, when R_θ is given, R_x' must be found by some iterative method such as Newton's. In a similar manner,

$$R_{\theta_i} = \frac{0.044\ R_{x_i}}{(\log R_{x_i} - 1.5)^2} \tag{41}$$

Once R_x' and R_{x_i} are found to satisfy Eqs. (40) and (41), C_f and C_{f_i} can be found from Eqs. (36) and (35) for $R_\theta = R_{\theta_i}$ and a new ratio of C_f/C_{f_i} can be determined. Such a ratio is shown in Fig. 3 along with experimental data from Refs. 10, 11, 18, 19, and 20. Again, good correlation is shown, indicating that Eq. (36) is satisfactory for the determination of C_f.

DETERMINATION OF H_i

As shown previously by Eq. (13), the transformed form factor can be expressed in terms of the incompressible, adiabatic form factor and temperature ratios. It is further shown in Appendix B that H_i is related to C_{f_i} by

$$H_i = \frac{1}{1 - 7\sqrt{C_{f_i}/2}} \tag{42}$$

and is, therefore, a function of the incompressible Reynolds number. Thus, there remains the problem of determining the relation between the compressible and incompressible Reynolds number.

In the transformation of Eq. (3) into Eq. (8) by means of Eq. (6) and (7), no transformation of x was involved. However, Eq. (8) can be written as

$$\frac{d\theta_{tr}}{dX} + \frac{\theta_{tr}}{U_e}\frac{dU_e}{dX}(2 + H_{tr}) + \frac{\theta_{tr}}{r}\frac{dr}{dX} = \frac{dx}{dX}\frac{C_f}{2}\sec\omega\left(\frac{T_e}{T_o}\right)^{\frac{\gamma+1}{2(\gamma-1)}} \tag{43}$$

where U_e is the transformed velocity (Appendix A) and the transformation dx/dX must be defined. For incompressible flow, the momentum equation can be written as

$$\frac{d\theta_i}{dx_i} + \frac{\theta_i}{u_{e_i}}\frac{du_{e_i}}{dx_i}(2 + H_i) + \frac{\theta_i}{r}\frac{dr}{dx_i} = \frac{C_{f_i}}{2}\sec\omega \tag{44}$$

with fluid properties ρ_o and μ_o evaluated at T_o. Comparison of these equations indicates that the transformed flow may be considered incompressible if

$$\frac{dX}{dx} = \frac{C_f}{C_{f_i}}\left(\frac{T_e}{T_o}\right)^{\frac{\gamma+1}{2(\gamma-1)}} \tag{45}$$

where C_f is obtained as a function of Reynolds number based on x and C_{f_i} is obtained as a function of $R_X = \rho_o U_e X/\mu_o$.

The original Stewartson's transformation used the relation

$$\frac{dX}{dx} = \left(\frac{T_e}{T_o}\right)^{\frac{3\gamma-1}{2(\gamma-1)}} = \left(\frac{T_e}{T_o}\right)^4 \text{ for } \gamma = 1.4 \tag{46}$$

Culick and Hill (Ref. 21) using the stagnation temperature as a reference temperature obtained the relation

$$\frac{dX}{dx} = \left(\frac{T_e}{T_o}\right)^{\frac{\gamma+1}{2(\gamma-1)}+\frac{N-1}{N}} = \left(\frac{T_e}{T_o}\right)^{4-\frac{1}{N}} \text{ for } \gamma = 1.4 \tag{47}$$

Mager (Ref. 22) using a still different approach obtained the relation

$$\frac{dX}{dx} = \frac{\mu_e}{\mu_o}\left(\frac{T_e}{T_o}\right)^{\frac{\gamma+1}{2(\gamma-1)}} = \frac{\mu_e}{\mu_o}\left(\frac{T_e}{T_o}\right)^3 \text{ for } \gamma = 1.4 \tag{48}$$

which reduces to Stewartson's transformation if the viscosity is assumed proportional to the temperature.

If Eqs. (35) and (36) are substituted into Eq. (45), the result is, since $R_X = R_{x_i}$,

$$\frac{\mu_o}{\rho_o U_e}\frac{(\log R_X - 2.3686)}{(\log R_X - 1.5)^3}dR_X = \left(\frac{T_e}{T_o}\right)^{\frac{\gamma+1}{2(\gamma-1)}}\frac{T_e}{T'}\frac{(\log R_x' - 2.3686)}{(\log R_x' - 1.5)^3}\frac{\mu'}{\rho' u_e}dR_x' \tag{49}$$

which, after integrating, yields

$$\frac{\mu_o R_X}{\rho_o U_e (\log R_X - 1.5)^2} = \left(\frac{T_e}{T_o}\right)^{\frac{\gamma+1}{2(\gamma-1)}} \frac{T_e}{T'} \frac{\mu' R_x'}{\rho' u_e (\log R_x' - 1.5)^2} \tag{50}$$

Since

$$\frac{U_e}{u_e} = \left(\frac{T_o}{T_e}\right)^{1/2}, \quad \frac{\rho_o}{\rho_e} = \left(\frac{T_o}{T_e}\right)^{\frac{1}{\gamma-1}}, \text{ and } \quad \frac{\rho_e}{\rho'} = \frac{T'}{T_e}$$

Eq. (50) reduces to

$$\frac{R_X}{(\log R_X - 1.5)^2} = \frac{\mu'}{\mu_o} \frac{R_x'}{(\log R_x' - 1.5)^2} \tag{51}$$

which relates the incompressible Reynolds number to the reference Reynolds number. Eq. (51) cannot be solved directly for R_X, but the use of Newton's approximation with $R_X = (\mu'/\mu_o)R_x'$ as the first approximation yields as a second approximation

$$R_X = \frac{\frac{\mu' R_x'}{\mu_o}}{\left(\log \frac{\mu' R_x'}{\mu_o} - 2.3686\right)} \left[\frac{\left(\log \frac{\mu' R_x'}{\mu_o} - 1.5\right)^3}{(\log R_x' - 1.5)^2} - 0.8686\right] \tag{52}$$

which is sufficiently accurate to determine C_{f_i} from Eq. (35). This value of C_{f_i} is then used in Eq. (42) to determine H_i, after which H_{tr} can be found from Eq. (13) for use in integrating Eq. (10).

APPLICATION TO AXISYMMETRIC TUNNELS

In the application of Eq. (10) to calculate the boundary layer growth of an axisymmetric wind tunnel, the calculations are usually begun at the throat where the Mach number is unity. Equation (10) can thus be written

$$\left[\theta \frac{r}{r^*} \left(\frac{T_e}{T_o}\right)^{\frac{\gamma+1}{2(\gamma-1)}} M^{2+H_{tr}}\right]_x = \theta^* \left(\frac{T_e^*}{T_o}\right)^{\frac{\gamma+1}{2(\gamma-1)}} + \int_{x^*}^{x} \frac{r}{r^*} \left(\frac{T_e}{T_o}\right)^{\frac{\gamma+1}{2(\gamma-1)}} M^{2+H_{tr}} \frac{C_f}{2} \sec \omega \, dx \tag{53}$$

In many cases, the momentum thickness at the throat θ^* can be assumed to be equal to zero without appreciably affecting the values calculated near the end of the nozzle.

The Reynolds number at the throat must be based upon a value of x which is other than zero in order to start with a finite value of C_f. A useful approximation for this initial value of x^* can be obtained in the manner suggested by Sibulkin in Ref. 23. The velocity gradient at the throat is obtained in terms of the radius of curvature at the throat:

$$\left[\frac{du_e}{dx}\right]_{M=1} = \frac{a_o}{\frac{\gamma+1}{2}\sqrt{r^* R^*}} \tag{54}$$

It is then assumed that the velocity gradient is constant from zero to the throat so that

$$\frac{[u_e]_{M=1}}{x^*} = \frac{a_o}{\sqrt{\frac{\gamma+1}{2}}\, x^*} = \left[\frac{du_e}{dx}\right]_{M=1} \tag{55}$$

Therefore,

$$x^* = \sqrt{\frac{\gamma+1}{2} r^* R^*} \tag{56}$$

The Reynolds number at each point along the nozzle is thus based upon a value of x equal to x^* plus the distance from the throat to the point. In general, the distance s along the nozzle contour may be assumed to be equal to the distance x along the axis for the purpose of determining the Reynolds number.

The above approximation can also be used to estimate the momentum thickness at the throat with the additional assumption that the values of the reference temperature and the reference Reynolds number are constant and equal to the values at the throat. Equation (10) may then be written

$$\theta^* \left(\frac{T_e^*}{T_o}\right)^{\frac{\gamma+1}{2(\gamma-1)}} = \frac{T_o}{T^{*\prime}} \frac{C_f'}{2} \int_o^1 \frac{r}{r^*} \left(\frac{T_e}{T_o}\right)^{\frac{\gamma+1}{2(\gamma-1)}+1} M^{2+H_{tr}} \frac{du_e/dM}{du_e/dx}\, dM \tag{57}$$

Since

$$\frac{r}{r^*} = \left[\frac{1+\frac{\gamma-1}{2}M^2}{\frac{\gamma+1}{2}}\right]^{\frac{\gamma+1}{4(\gamma-1)}} \Big/ M^{1/2} \tag{58}$$

and

$$\frac{du_e}{dM} = \frac{a_o}{\left(1 + \frac{\gamma - 1}{2} M^2\right)^{3/2}} \tag{59}$$

thus, after substitution and rearranging,

$$\theta^* = \frac{0.044\,(\log R_{x^*}' - 2.3686)\, T_o \sqrt{r^* R^*} \left(\frac{\gamma+1}{2}\right)^{\frac{5\gamma-3}{4(\gamma-1)}}}{(\log R_{x^*}' - 1.5)^3\, T^{*\prime}} \int_o^1 \frac{M^{1.5 + H_{tr}}\, dM}{\left(1 + \frac{\gamma-1}{2} M^2\right)^{\frac{11\gamma-9}{4(\gamma-1)}}} \tag{60}$$

or, when $\gamma = 1.4$,

$$\theta^* = \frac{0.0694(\log R_{x^*}' - 2.3686)\, T_o \sqrt{r^* R^*}}{(\log R_{x^*}' - 1.5)^3\, T^{*\prime}} \int_o^1 \frac{M^{1.5 + H_{tr}}\, dM}{(1 + 0.2 M^2)^4} \tag{61}$$

The integration indicated in Eq. (61) can be performed analytically for values of H_{tr} which are odd multiples of 0.5. For intermediate values, the integration must be performed numerically. The results of such integrations are shown in Fig. 4.

For conical nozzles in which radial flow can be assumed, the Mach number is constant over each spherical segment of area $2\pi r^2/(1 + \cos \omega)$. Since the throat area is πr^{*2},

$$\frac{A}{A^*} = \frac{2r^2}{(1 + \cos \omega)\, r^{*2}} = \frac{1}{M} \left[\frac{1 + \frac{\gamma-1}{2} M^2}{\frac{\gamma+1}{2}}\right]^{\frac{\gamma+1}{2(\gamma-1)}} \tag{62}$$

or

$$\frac{r}{r^*} = \sqrt{\frac{1 + \cos \omega}{2M}} \left[\frac{1 + \frac{\gamma-1}{2} M^2}{\frac{\gamma+1}{2}}\right]^{\frac{\gamma+1}{4(\gamma-1)}} \tag{63}$$

from which

$$\frac{dr}{dM} = \frac{r^*}{2} \sqrt{\frac{1 + \cos \omega}{2M^3}}\, \frac{(M^2 - 1)\left(1 + \frac{\gamma-1}{2} M^2\right)^{\frac{5-3\gamma}{4(\gamma-1)}}}{\left(\frac{\gamma+1}{2}\right)^{\frac{\gamma+1}{4(\gamma-1)}}} \tag{64}$$

Then, since $dr/dx = \tan \omega$

$$dx = \frac{r^*}{2} \sqrt{\frac{1 + \cos \omega}{2 M^3}} \; \frac{(M^2 - 1)\left(1 + \frac{\gamma - 1}{2} M^2\right)^{\frac{5 - 3\gamma}{4(\gamma - 1)}} \cot \omega}{\left(\frac{\gamma + 1}{2}\right)^{\frac{\gamma + 1}{4(\gamma - 1)}}} \, dM \tag{65}$$

Substituting Eqs. (63) and (65) into Eq. (10) yields

$$\left[\theta \frac{r}{r^*} \left(\frac{T_e}{T_o}\right)^{\frac{\gamma + 1}{2(\gamma - 1)}} M^{2 + H_{tr}}\right]_b = \left[\theta \frac{r}{r^*} \left(\frac{T_e}{T_o}\right)^{\frac{\gamma + 1}{2(\gamma - 1)}} M^{2 + H_{tr}}\right]_a + \frac{r^* (1 + \cos \omega) \csc \omega}{4\left(\frac{\gamma + 1}{2}\right)^{\frac{\gamma + 1}{2(\gamma - 1)}}} \int_a^b \frac{(M^2 - 1) M^{H_{tr}} C_f/2}{1 + \frac{\gamma - 1}{2} M^2} \, dM \tag{66}$$

As before, if the reference temperature and reference Reynolds number can be assumed to be constant,

$$\left[\theta \frac{r}{r^*} \left(\frac{T_e}{T_o}\right)^{\frac{\gamma + 1}{2(\gamma - 1)}} M^{2 + H_{tr}}\right]_b = \left[\theta \frac{r}{r^*} \left(\frac{T_e}{T_o}\right)^{\frac{\gamma + 1}{2(\gamma - 1)}} M^{2 + H_{tr}}\right]_a + \frac{r^* (1 + \cos \omega) \csc \omega \, T_o \, C_f'}{8\left(\frac{\gamma + 1}{2}\right)^{\frac{\gamma + 1}{2(\gamma - 1)}} T'} \int_a^b \frac{(M^2 - 1) M^{H_{tr}}}{\left(1 + \frac{\gamma - 1}{2} M^2\right)^2} \, dM \tag{67}$$

and, if $\gamma = 1.4$,

$$\left[\theta \frac{r}{r^*} \left(\frac{T_e}{T_o}\right)^3 M^{2 + H_{tr}}\right]_b = \left[\theta \frac{r}{r^*} \left(\frac{T_e}{T_o}\right)^3 M^{2 + H_{tr}}\right]_a + \frac{0.00637 (\log R_x' - 2.3686) \, T_o \, r^* \cot \frac{\omega}{2}}{(\log R_x' - 1.5)^3 \, T'} \int_a^b \frac{(M^2 - 1) M^{H_{tr}} \, dM}{(1 + 0.2 M^2)^2} \tag{68}$$

The integration indicated in Eq. (68) can be performed analytically when H_{tr} is an integer and numerically when H_{tr} is not an integer. The results of such integrations are shown in Fig. 5 where the integration in each case is performed, for convenience, over the interval from 1 to M. Obviously,

$$\int_a^b f(M) \, dM = \int_1^b f(M) \, dM - \int_1^a f(M) \, dM$$

For the general case of conical and contoured nozzles, the reference temperature and Reynolds number are not constant, and for the contoured nozzle the radius is not an analytic function of the Mach number. Equation (53) must therefore be used downstream of the throat while Eq. (60) or (61) can be used to estimate the value at the throat. In many cases, the variation of R_χ over the length of the nozzle is small enough that a constant average value of H_i can be used and the computations involved can thereby be simplified.

Values of boundary-layer displacement thickness calculated by the method described are compared with experimental values in Figs. 6 and 7 for Mach 7 and 8 conical nozzles and in Fig. 8 for a Mach 8 contoured nozzle. The experimental data were obtained in the 50-inch-diameter nozzles of the Gas Dynamics Facility. The agreement shown is considered to be extremely good.

CONCLUDING REMARKS

A method has been developed for calculating the growth of a turbulent boundary layer at hypersonic Mach numbers. Excellent agreement with experimental results from axisymmetric nozzles has been obtained through the application of this method. The basis for the calculations is Eq. (10) wherein the compressible skin-friction coefficient is obtained from Eq. (36), and the transformed form factor is given by Eq. (13) in which the incompressible form factor is related by Eq. (42) to the incompressible skin-friction coefficient evaluated at the incompressible Reynolds number given by Eq. (52).

APPENDIX A

STEWARTSON'S TRANSFORMATION

In the Stewartson's transformation, as given in Ref. 9, the distance normal to the surface is transformed by the relation

$$dY = \frac{\rho}{\rho_o} \frac{a_e}{a_o} dy \tag{A-1}$$

and the velocity parallel to the surface is transformed by the relation

$$U = u \frac{a_o}{a_e} \tag{A-2}$$

External of the boundary layer

$$U_e = u_e \frac{a_o}{a_e} \tag{A-3}$$

so that

$$\frac{U}{U_e} = \frac{u}{u_e} \tag{A-4}$$

The definition of boundary-layer momentum thickness is

$$\theta = \int_o^\Delta \frac{\rho u}{\rho_e u_e} \left(1 - \frac{u}{u_e}\right) dy \tag{A-5}$$

where Δ is the value of y where both velocity and temperature reach their free-stream values. Substitution of Eqs. (A-1) and (A-4) into Eq. (A-5) yields

$$\theta = \frac{\rho_o a_o}{\rho_e a_e} \int_o^\Delta \frac{U}{U_e} \left(1 - \frac{U}{U_e}\right) dY \tag{A-6}$$

The transformed momentum thickness is defined as

$$\theta_{tr} = \int_o^\Delta \frac{U}{U_e} \left(1 - \frac{U}{U_e}\right) dY \tag{A-7}$$

so that

$$\theta = \frac{\rho_o a_o}{\rho_e a_e} \theta_{tr} \tag{A-8}$$

or

$$\theta = \theta_{tr}\left(1 + \frac{\gamma - 1}{2} M^2\right)^{\frac{\gamma+1}{2(\gamma-1)}} = \theta_{tr}\left(\frac{T_o}{T_e}\right)^{\frac{\gamma+1}{2(\gamma-1)}} \tag{A-9}$$

It may be noted that Eq. (A-7) has the form for incompressible flow, although the shape of the velocity profile is distorted by the transformation (see Ref. 24).

In a similar manner, the boundary-layer displacement thickness is defined by the equation

$$\delta^* = \int_o^\Lambda \left(1 - \frac{\rho\, u}{\rho_e\, u_e}\right) dy \tag{A-10}$$

Since the pressure is assumed to be constant through the boundary layer, Eq. (A-10) may be written as

$$\delta^* = \int_o^\Lambda \frac{\rho}{\rho_e}\left(\frac{T}{T_e} - \frac{u}{u_e}\right) dy \tag{A-11}$$

The static temperature distribution through the boundary layer may be expressed by

$$\frac{T}{T_e} = \frac{T_s}{T_o}\left(1 + \frac{\gamma - 1}{2} M^2\right) - \frac{\gamma - 1}{2} M^2 \left(\frac{u}{u_e}\right)^2 \tag{A-12}$$

where T_s is the local stagnation temperature corresponding to the local static temperature T. Substituting Eqs. (A-1), (A-4), and (A-12) into Eq. (A-11) yields

$$\delta^* = \frac{\rho_o\, a_o}{\rho_e\, a_e} \int_o^\Lambda \left[\left(1 + \frac{\gamma - 1}{2} M^2\right)\left(\frac{T_s}{T_o} - \frac{U}{U_e}\right) + \frac{\gamma - 1}{2} M^2 \frac{U}{U_e}\left(1 - \frac{U}{U_e}\right)\right] dY \tag{A-13}$$

or

$$\delta^* = \frac{\rho_o\, a_o}{\rho_e\, a_e}\left[\left(1 + \frac{\gamma - 1}{2} M^2\right)\delta_{tr}^* + \frac{\gamma - 1}{2} M^2\, \theta_{tr}\right] \tag{A-14}$$

where, by definition

$$\delta_{tr}^* = \int_o^\Delta \left(\frac{T_s}{T_o} - \frac{U}{U_e}\right) dY \tag{A-15}$$

When T_s is constant and equal to T_o, Eq. (A-15) has the form for incompressible flow.

Division of Eq. (A-14) by Eq. (A-8) yields

$$\frac{\delta^*}{\theta} = \left(1 + \frac{\gamma - 1}{2} M^2\right) \frac{\delta_{tr}^*}{\theta_{tr}} + \frac{\gamma - 1}{2} M^2 \tag{A-16}$$

or

$$H = H_{tr}\left(1 + \frac{\gamma - 1}{2} M^2\right) + \frac{\gamma - 1}{2} M^2 \tag{A-17}$$

Equations (A-9) and (A-17) were used to transform Eq. (3). Equation (A-15) may be written as

$$\delta_{tr}^* = \int_o^\Delta \left[\left(\frac{T_s}{T_o} - 1\right) + \left(1 - \frac{U}{U_e}\right)\right] dY \tag{A-18}$$

so that

$$H_{tr} = \frac{1}{\theta_{tr}} \int_o^\Delta \left(\frac{T_s}{T_o} - 1\right) dY + H_i \tag{A-19}$$

where

$$H_i = \frac{1}{\theta_{tr}} \int_o^\Delta \left(1 - \frac{U}{U_e}\right) dY \tag{A-20}$$

In order to evaluate Eq. (A-19), use is made of Crocco's quadratic temperature distribution, written as in Ref. 8,

$$\frac{T}{T_e} = \frac{T_w}{T_e} - \left(\frac{T_w - T_{aw}}{T_e}\right)\left(\frac{u}{u_e}\right) - \left(\frac{T_{aw} - T_e}{T_e}\right)\left(\frac{u}{u_e}\right)^2 \tag{A-21}$$

which assumes that the thermal boundary layer has the same thickness as the velocity boundary layer. This would occur only if the Prandtl number is unity. However, Eq. (A-21) partially accounts for Prandtl numbers other than unity through the use of the adiabatic wall temperature instead of the stagnation temperature. Substitution of Eq. (A-21) into Eq. (A-11), along with Eqs. (A-1) and (A-4) yields

$$\delta^* = \frac{\rho_o a_o}{\rho_e a_e} \int_o^\Delta \left[\frac{T_w}{T_e}\left(1 - \frac{U}{U_e}\right) + \left(\frac{T_{aw}}{T_e} - 1\right) \frac{U}{U_e}\left(1 - \frac{U}{U_e}\right)\right] dY \tag{A-22}$$

or

$$\delta^* = \frac{\rho_o\, a_o}{\rho_e\, a_e}\left[\frac{T_w}{T_e}\int_o^{\Delta}\left(1 - \frac{U}{U_e}\right) dY + \left(\frac{T_{aw}}{T_e} - 1\right)\theta_{tr}\right] \qquad \text{(A-23)}$$

Division of Eq. (A-23) by (A-8) yields

$$H = \frac{T_w}{T_e} H_i + \frac{T_{aw}}{T_e} - 1 \qquad \text{(A-24)}$$

Equations (A-24) and (A-17) may be combined so that

$$H_{tr} = H_i \frac{T_w}{T_o} + \frac{T_{aw}}{T_o} - 1 \qquad \text{(A-25)}$$

The variation of H according to Eq. (A-24) as a function of Mach number is compared in Fig. 9 with experimental results from Refs. 10 and 25 and in Fig. 10 with the tabulated results from Ref. 26. The correlation is considered to be very good and justifies the derivation described.

APPENDIX B

INCOMPRESSIBLE SKIN-FRICTION COEFFICIENTS

A great many empirical equations have been developed for the variation of the local and mean skin-friction coefficients with Reynolds number for incompressible flow. Probably the most simple to use are the power-law equations

$$\frac{C_{f_i}}{2} = \frac{\alpha}{\left(R\theta_i\right)^{\frac{1}{N}}} \tag{B-1}$$

$$\frac{C_{f_i}}{2} = \frac{\beta}{\left(R_{x_i}\right)^{\frac{1}{N+1}}} \tag{B-2}$$

$$\frac{C_{F_i}}{2} = \frac{R\theta_i}{R_{x_i}} = \frac{N+1}{N} \cdot \frac{C_{f_i}}{2} \tag{B-3}$$

where

$$\beta = \frac{\alpha^{\frac{N}{N+1}}}{\left(\frac{N+1}{N}\right)^{\frac{1}{N+1}}} \tag{B-4}$$

For a limited range of Reynolds numbers, values of α, β, and N can be considered to be constant; but, for a large range of Reynolds numbers, their values must also be functions of the Reynolds number.

Locke (Ref. 27) investigated a number of the empirical equations and found that Schoenherr's equation

$$\frac{0.242}{\sqrt{C_{F_i}}} = \log\left(C_{F_i} R_{x_i}\right) \tag{B-5}$$

gave a good correlation with a very large amount of experimental data over the wide range of Reynolds numbers from 10^5 to 10^9. Other forms of this equation are

$$\frac{0.242}{\sqrt{C_{F_i}}} = \log\left(2 R\theta_i\right) \tag{B-6}$$

and

$$C_{f_i} = \frac{(0.242)^2}{\log(2R\theta_i)\left[\log(2R\theta_i) + 0.8686\right]} \tag{B-7}$$

Although Schoenherr's equations correlate well with experimental results, they are difficult to use because neither C_{f_i} or C_{F_i} can be found directly as a function of R_{x_i}. Tables can be constructed for use when the computing is done manually; however, more direct equations are desired for use with automatic computers. Any set of equations must satisfy the relationship

$$C_{f_i} = C_{F_i} + R_{x_i} \frac{d C_{F_i}}{d R_{x_i}} \tag{B-8}$$

or

$$C_{F_i} = \frac{1}{R_{x_i}} \int_o^{R_{x_i}} C_{f_i}\, dR_{x_i} \tag{B-9}$$

After an investigation of several types of equations, the equations

$$C_{F_i} = \frac{0.088}{(\log R_{x_i} - 1.5)^2} \tag{B-10}$$

and

$$C_{f_i} = \frac{0.088\,(\log R_{x_i} - 2.3686)}{(\log R_{x_i} - 1.5)^3} \tag{B-11}$$

were found to correlate with experimental data as well as Schoenherr's equations over the range of Reynolds numbers from 10^5 to 10^9. A comparison of values of C_{F_i} calculated from Eq. (B-10) with those from Eq. (B-5) is shown in Fig. 11 together with the "ideal" values from Ref. 28 and 29. A similar comparison of values of C_{f_i} is shown in Fig. 12 together with experimental values of Dhawan (Ref. 30), Schultz-Grunow (Ref. 31), and Kempf (Ref. 32). These data are recognized as being among the most accurately determined values available. A further comparison of $R\theta_i$ as a function of R_{x_i} is made in Fig. 13 with the experimental values of Wieghardt (Ref. 33). All of these comparisons indicate the validity of Eqs. (B-10) and (B-11).

A critical examination of the curve of Eq. (B-10) shows that it crosses Schoenherr's curve at a Reynolds number of about 10^5 and again at about 5×10^7. Moreover, it goes to infinity when $\log R_{x_i} = 1.5$ or $R_{x_i} = 32$. Furthermore, the curve of Eq. (B-11) has zero slope when

log R_{x_i} = 2.3686 or R_{x_i} = 234. Both of these conditions are well below the range for turbulent boundary layers and are, therefore, of academic interest only. The values of the constants, 0.088 and 1.5, could have been chosen to agree better with Coles' values but the experimental values do not warrant such a selection.

The incompressible form factor H_i is also a function of Reynolds number and is shown in Ref. 29 to be related to the skin-friction coefficient in the manner,

$$H_i = \frac{1}{1 - 7\sqrt{C_{f_i}/2}} \tag{B-12}$$

where the constant 7 (although different from that of Ref. 29) is chosen for correlation with experimental data. Such correlations are shown in Figs. 14 and 15. Again the correlations are quite satisfactory.

For comparative purposes, values of C_{F_i}, C_{f_i}, R_{θ_i}, and H_i are listed in Table 1 for various values of R_{x_i} from 10^5 to 10^9. Also listed are the values of N obtained from Eq. (B-3) which show that the use of Eqs. (B-1) and (B-2) must be limited to small ranges of Reynolds number.

REFERENCES

1. Granville, Paul S. "A Method for the Calculation of the Turbulent Boundary Layer in a Pressure Gradient." Rep. 752, Navy Dept., The David W. Taylor Model Basin (Washington, D.C.), May 1951.
2. Tetervin, Neal and Lin, Chia Chiao. "A General Integral Form of the Boundary-Layer Equation for Incompressible Flow with an Application to the Calculation of the Separation Point of Turbulent Boundary Layers." NACA Rept. 1046, 1951.
3. Tucker, Maurice. "Approximate Calculation of Turbulent Boundary-Layer Development in Compressible Flow." NACA TN 2337, April 1951.
4. Bartz, D. R. "An Approximate Solution of Compressible Turbulent Boundary-Layer Development and Convective Heat Transfer in Convergent-Divergent Nozzles." JPL CIT, Progress Report No. 20-234, July 1954.
5. Sommer, Simon C., and Short, Barbara J. "Free-Flight Measurements of Turbulent-Boundary-Layer Skin Friction in the Presence of Severe Aerodynamic Heating at Mach Numbers from 2.8 to 7.0." NACA TN 3391, March 1955.
6. Tendeland, Thorval. "Effects of Mach Number and Wall-Temperature Ratio on Turbulent Heat Transfer at Mach Numbers from 3 to 5." NACA TN 4236, April 1958.
7. Eckert, E.R.G. "Survey on Heat Transfer at High Speeds." WADC Technical Report 54-70, April 1954.
8. Persh, Jerome. "A Theoretical Investigation of Turbulent Boundary-Layer Flow with Heat Transfer at Supersonic and Hypersonic Speeds." NAVORD Report 3854, May 1955.
9. Reshotko, Eli and Tucker, Maurice. "Approximate Calculation of the Compressible Turbulent Boundary Layer with Heat Transfer and Arbitrary Pressure Gradient." NACA TN 4154, December 1957.
10. Coles, Donald. "Measurements in the Boundary Layer on a Smooth Flat Plate in Supersonic Flow, III. Measurements in a Flat-Plate Boundary Layer at the Jet Propulsion Laboratory." JPL Report No. 20-71, June 1953.
11. Lobb, L. K., Winkler, E. M, and Persh, Jerome. "NOL Hypersonic Tunnel No. 4 Results VII: Experimental Investigation of Turbulent Boundary Layers in Hypersonic Flow." NAVORD Report No. 3880, ARR 262, March 1955.

12. Chapman, Dean R. and Kester, Robert H. "Measurements of Turbulent Skin Friction on Cylinders in Axial Flow at Subsonic and Supersonic Velocities." Paper presented at 21st Meeting, I.A.S., New York, N.Y., January 26-29, 1953 (Preprint No. 391).

13. Fallis, W. B. "Heat Transfer in the Transitional and Turbulent Boundary Layers on Flat Plate at Supersonic Speeds." UTIA Rep 19, University of Toronto, May 1952.

14. Pappas, C. C. "Measurement of Heat Transfer in the Turbulent Boundary Layer on a Flat Plate in Supersonic Flow, and Comparison with Skin-Friction Results." NACA TN 3222, June 1954.

15. Humble, L. V., Lowdermilk, W. H., and Desman, L. G. "Measurements of Average Heat-Transfer and Friction Coefficients for Subsonic Flow of Air in Smooth Tubes at High Surface and Fluid Temperatures." NACA Report 1020, 1951.

16. De Coursin, D. G., Bradfield, W. S., and Sheppard, J. J. "Measurement of Turbulent Heat Transfer on Bodies of Revolution at Supersonic Speed." JAS 23, March 1956, pp 272-3. Also WADC Report 53-379, February 1954.

17. Monaghan, R. J. and Cooke, J. R. "The Measurement of Heat Transfer and Skin Friction at Supersonic Speeds." Part III "Measurements of Overall Heat Transfer and of the Associated Boundary Layers on a Flat Plate at $M_1 = 2.43$." Tech. Note AERO 2129, British R.A.E., December 1951.

18. Hill, F. K. "Boundary-Layer Measurements in Hypersonic Flow." JAS 23, January 1956, pp 35 - 42.

19. Korkegi, R. H. "Transition Studies and Skin-Friction Measurements on an Insulated Flat Plate at a Mach Number of 5.8." JAS 23, February 1956, pp 97 - 107, 192.

20. Brinich, P. F., and Diaconis, N. S. "Boundary-Layer Development and Skin Friction at Mach Number 3.05." NACA TN 2742, July 1952.

21. Culick, Fred E. C., and Hill, Jacques A. F. "A Turbulent Analog of the Stewartson - Illingworth Transformation." JAS 25, April 1958, pp 259 - 262.

22. Mager, Artur. "Transformation of the Compressible Turbulent Boundary Layer." JAS 25, May 1958, pp 305 - 311.

23. Sibulkin, Merwin. "Heat Transfer to an Incompressible Turbulent Boundary Layer and Estimation of Heat-Transfer Coefficients at Supersonic Nozzle Throats." JPL Report No. 20-78, July 1954.

24. Reshotko, Eli and Tucker, Maurice. "Effects of a Discontinuity on a Turbulent Boundary-Layer-Thickness Parameter with Application to Shock-Induced Separation." NACA TN 3454, May 1955.

25. Baron, Judson R. "Analytic Design of a Family of Supersonic Nozzles by the Friedrichs Method." WADC TR 54-279, June 1954.

26. "Tabulation of Compressible Turbulent-Boundary-Layer Parameters." NAVORD Report No. 4282, May 1956.

27. Locke, F. W. S., Jr. "Navaer Recommended Definition of Turbulent Friction in Incompressible Fluids." Bureau of Aeronautics, Navy Dept., DR Report No. 1415, June 1952.

28. Smith, Donald W. and Walker, John H. "Skin Friction Measurements in Incompressible Flow." NACA TN 4231, March 1958.

29. Coles, Donald. "Measurements in the Boundary Layer on a Smooth Flat Plate in Supersonic Flow, I. The Problem of the Turbulent Boundary Layer." JPL Report No. 20-69, June 1953.

30. Dhawan, Satish. "Direct Measurements of Skin Friction." NACA Report No. 1121, 1953 (Supersedes NACA TN 2567).

31. Schultz-Grunow, F. "New Frictional Resistance Law for Smooth Plates." NACA TM 986, 1940.

32. Kempf, von Gunther. "Neue Ergebnisse der Widerstandsforschung." Werft, Reederei, Hafen, Vol. 10, No. 11, pp 234-239; No. 12 pp 247-253, 1929.

33. Wieghardt, K. "Zum Reibungswiderstand rauher Platten." ZWB, KWI, U and M 6612, Sept. 1944. See also "Uber die turbulente Strömung im Rohr und längs einer Platte." ZAMM, Vol. 24, No. 5/6, pp 294-296, 1944.

34. Hama, F. R. "The Turbulent Boundary Layer Along a Flat Plate, I and II." (in Japanese) Reports of the Institute of Science and Technology, Tokyo Imperial University, Vol. I, No. 1, pp 13 - 16. No. 3 - 4, pp 49 - 50, 1947.

TABLE 1

INCOMPRESSIBLE SKIN FRICTION VALUES

R_{x_i}	C_{f_i}	C_{F_i}	R_{θ_i}	H_i	N
10^5	.005401	.007184	359.2	1.5726	3.03
2×10^5	.004699	.006091	609.1	1.5135	3.38
3×10^5	.004348	.005564	834.5	1.4845	3.58
4×10^5	.004122	.005230	1046.0	1.4658	3.72
5×10^5	.003959	.004991	1248.0	1.4523	3.83
6×10^5	.003832	.004808	1442.0	1.4418	3.93
7×10^5	.003731	.004662	1632.0	1.4334	4.00
8×10^5	.003644	.004539	1816.0	1.4261	4.07
9×10^5	.003571	.004435	1996.0	1.4200	4.13
10^6	.003507	.004346	2173.0	1.4147	4.18
2×10^6	.003127	.003818	3818.0	1.3827	4.53
3×10^6	.002986	.003596	5393.0	1.3707	4.73
4×10^6	.002805	.003381	6761.0	1.3553	4.87
5×10^6	.002712	.003256	8139.0	1.3473	4.99
6×10^6	.002639	.003159	9476.0	1.3410	5.08
7×10^6	.002580	.003080	10780.0	1.3359	5.15
8×10^6	.002530	.003014	12060.0	1.3315	5.22
9×10^6	.002487	.002958	13310.0	1.3277	5.28
10^7	.002450	.002909	14550.0	1.3245	5.33
2×10^7	.002223	.002615	26150.0	1.3044	5.68
3×10^7	.002105	.002463	36950.0	1.2938	5.88
4×10^7	.002027	.002363	47270.0	1.2868	6.03
5×10^7	.001969	.002290	57250.0	1.2815	6.14
6×10^7	.001924	.002233	66980.0	1.2773	6.23
7×10^7	.001887	.002186	76500.0	1.2739	6.31
8×10^7	.001855	.002146	85850.0	1.2709	6.37
9×10^7	.001828	.002112	95060.0	1.2684	6.43
10^8	.001805	.002083	104100.0	1.2663	6.48
2×10^8	.001660	.001903	190300.0	1.2526	6.83
4×10^8	.001531	.001745	348900.0	1.2402	7.18
6×10^8	.001463	.001661	498400.0	1.2335	7.38
8×10^8	.001417	.001606	642300.0	1.2290	7.52
10^9	.001383	.001564	782200.0	1.2256	7.63

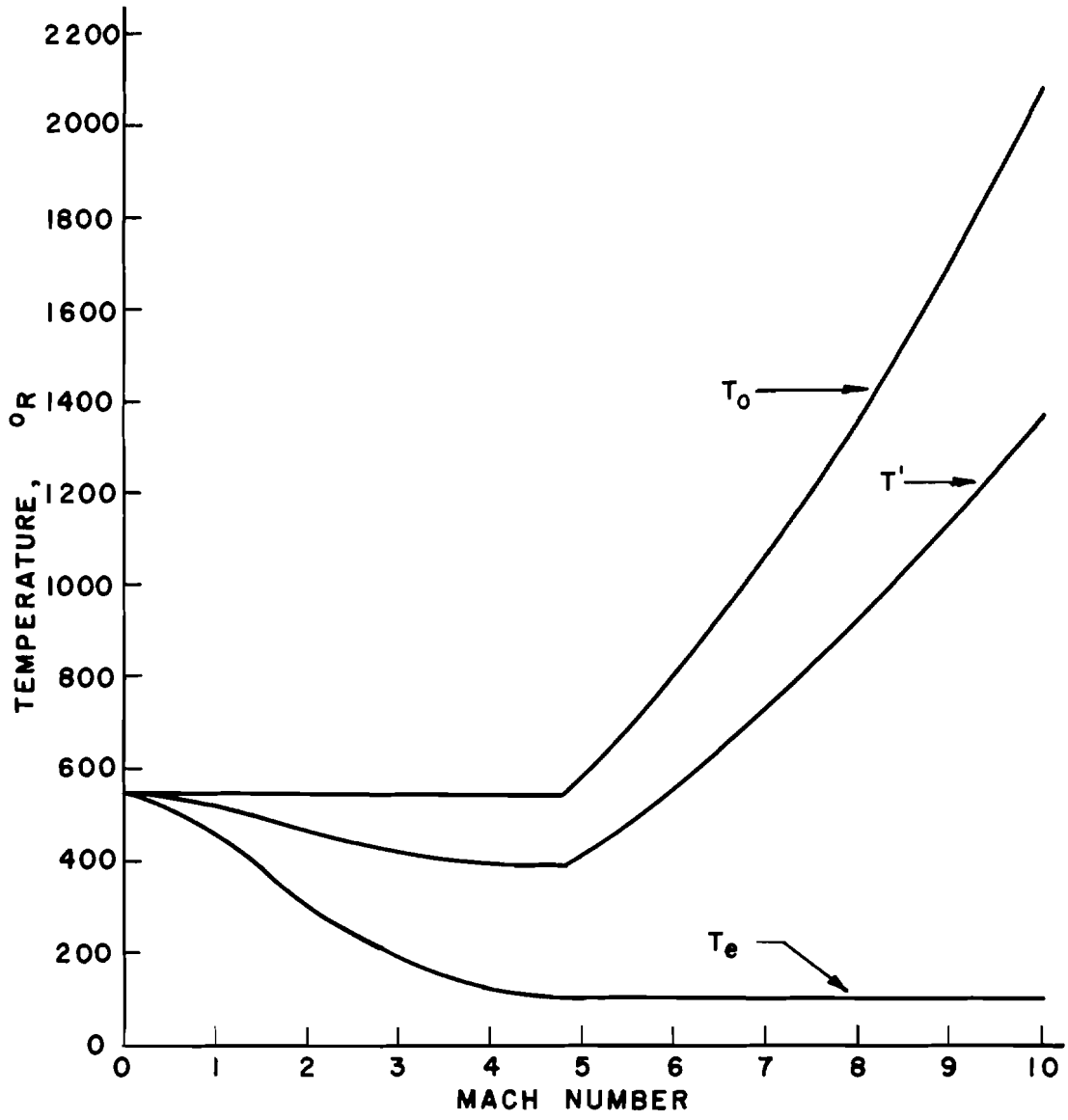

Fig. 1 Temperature Variations Used for Correlating Wind Tunnel Results

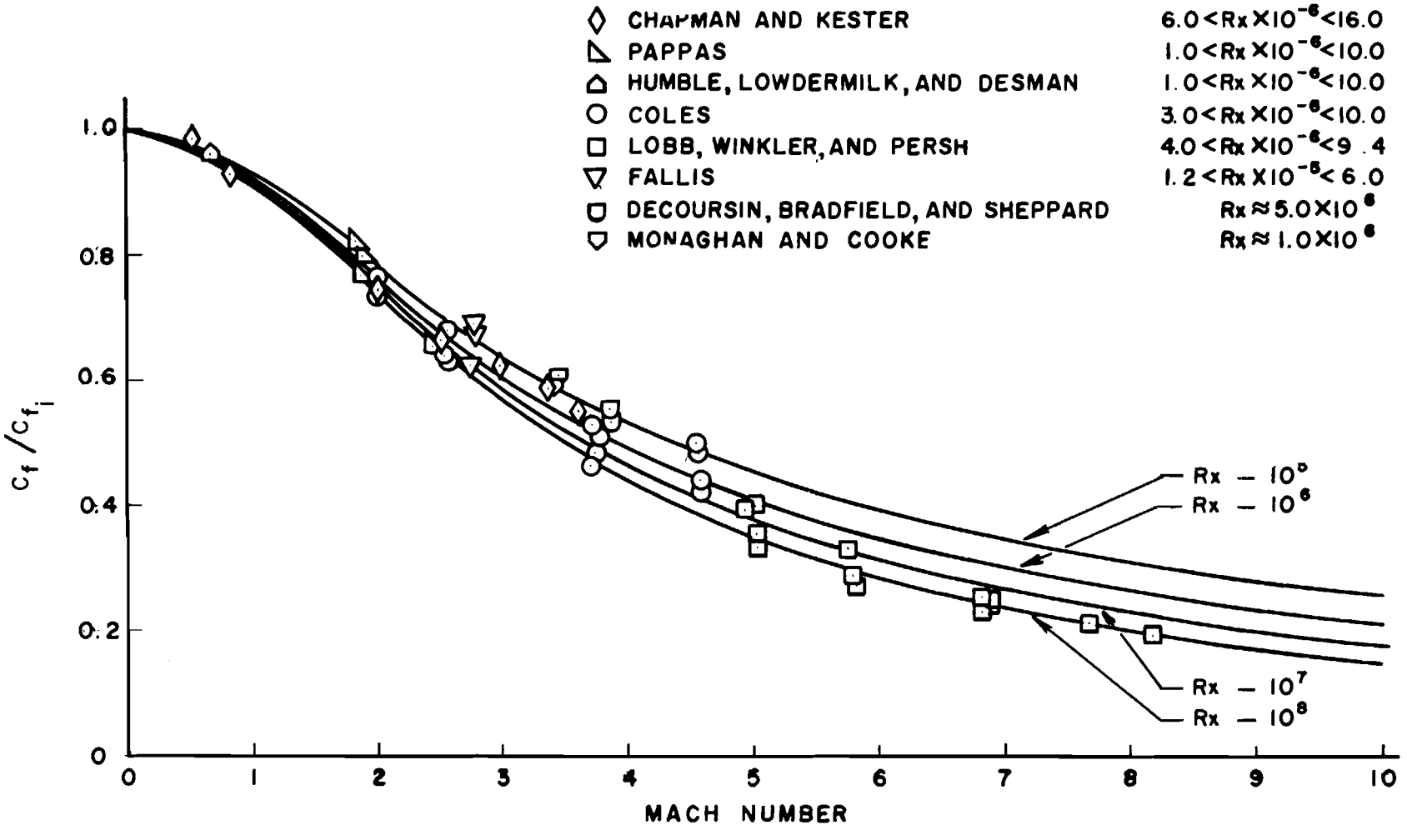

Fig. 2 Correlation of Calculated Ratios, C_f/C_{f_i}, with Experimental Values Based upon R_x

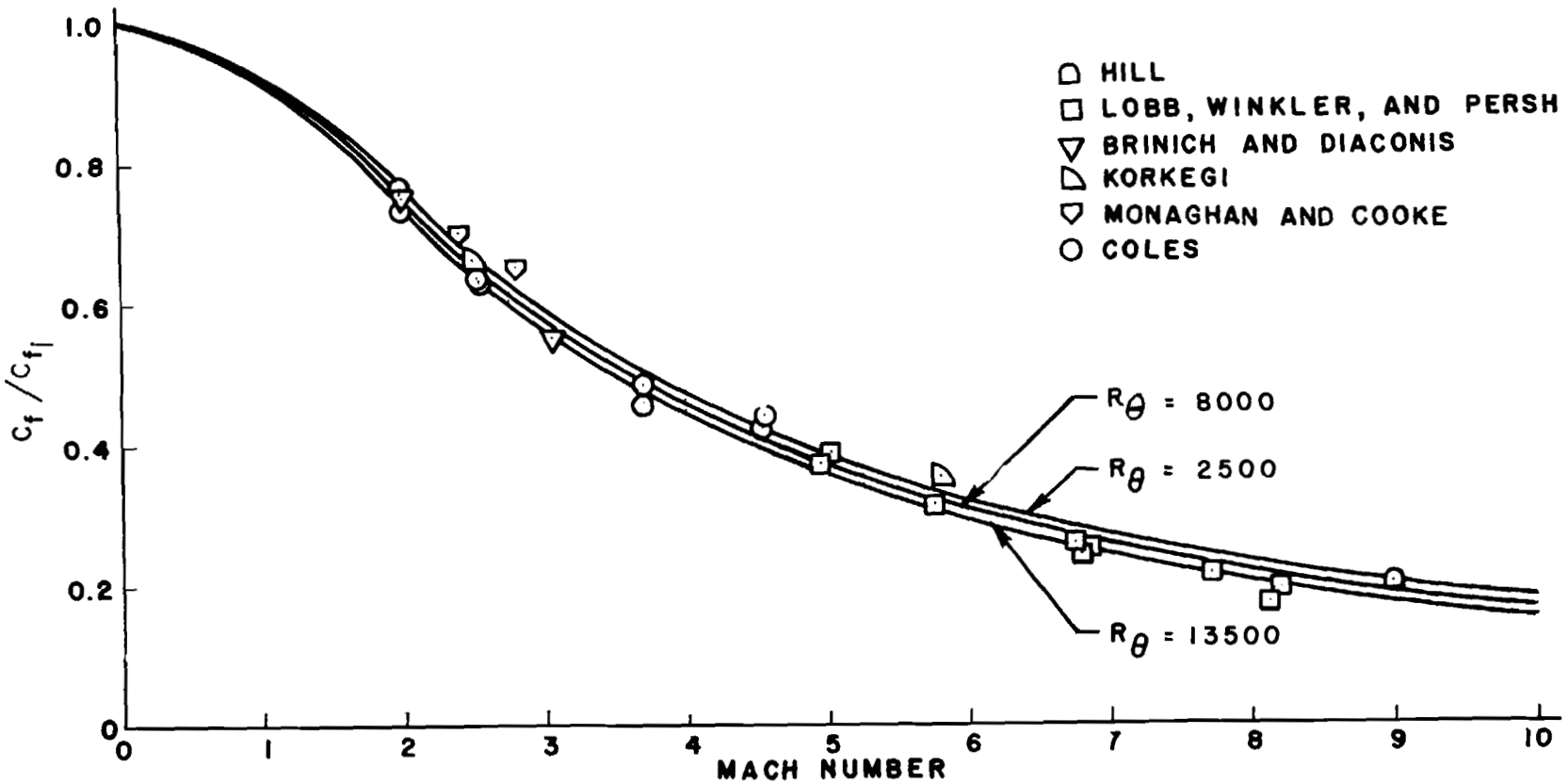

Fig. 3 Correlation of Calculated Ratios, C_f/C_{f_i}, with Experimental Values Based upon R_θ

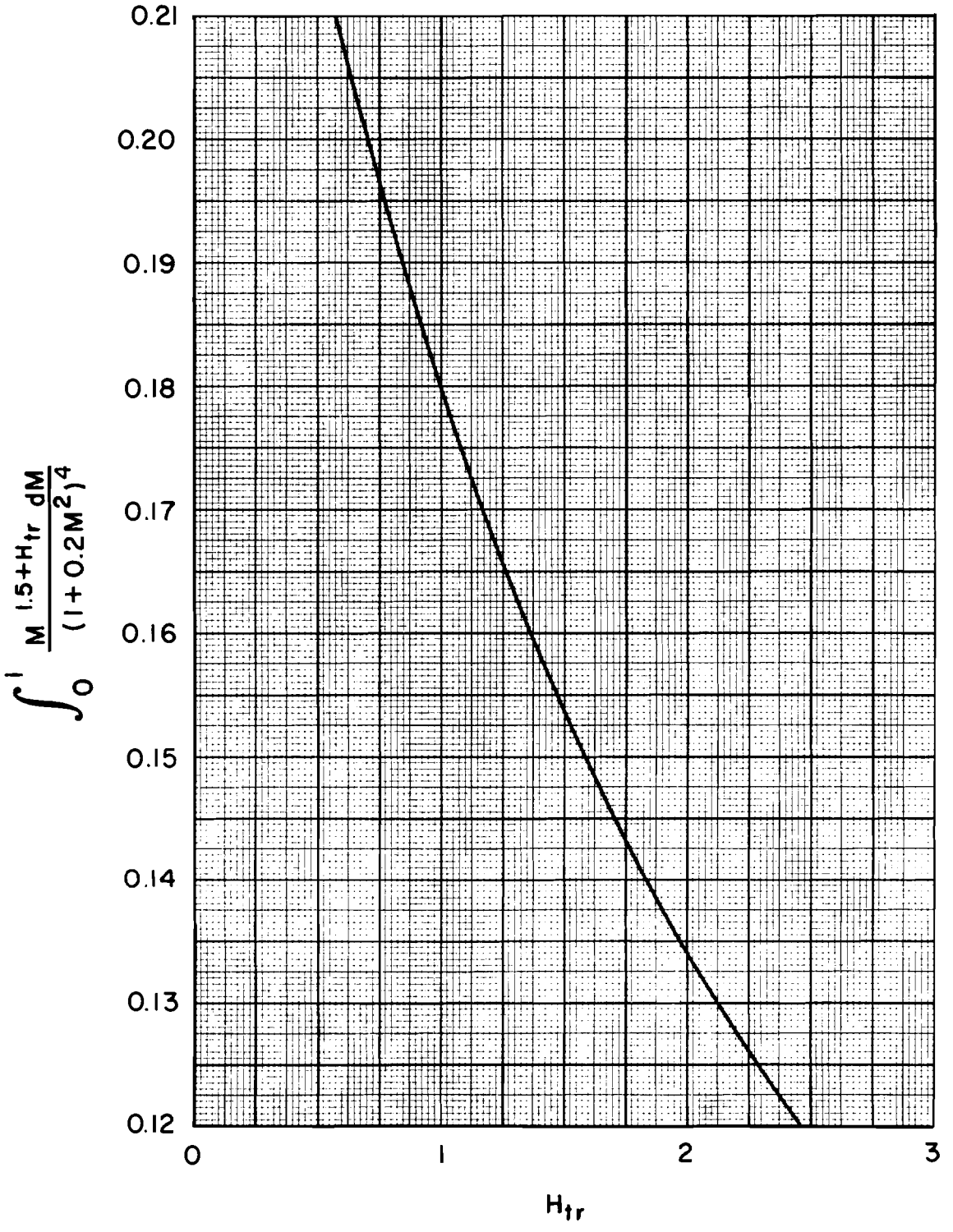

Fig. 4 Values of Integral Used in Calculating Boundary-Layer Thickness at the Throat of an Axisymmetric Nozzle

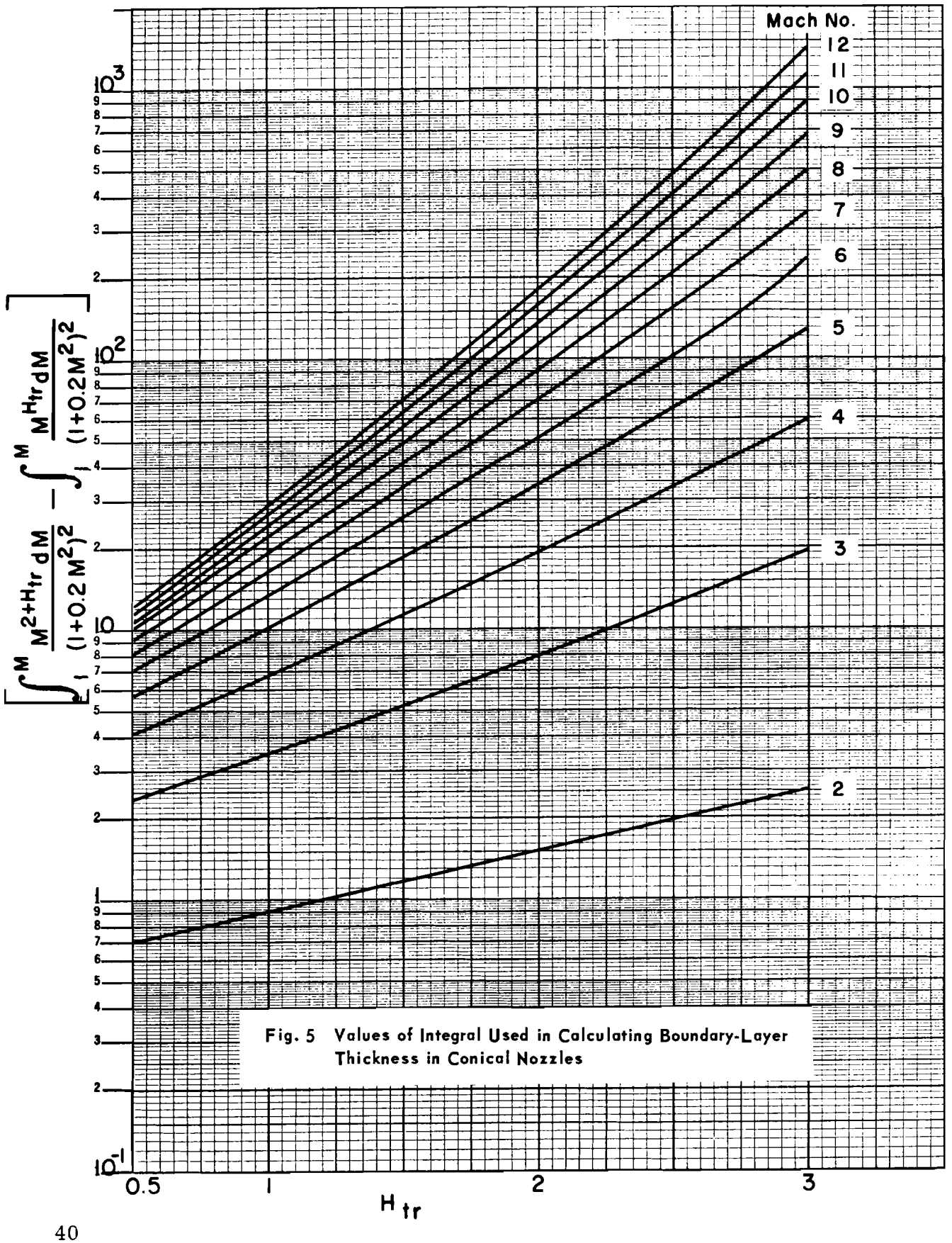

Fig. 5 Values of Integral Used in Calculating Boundary-Layer Thickness in Conical Nozzles

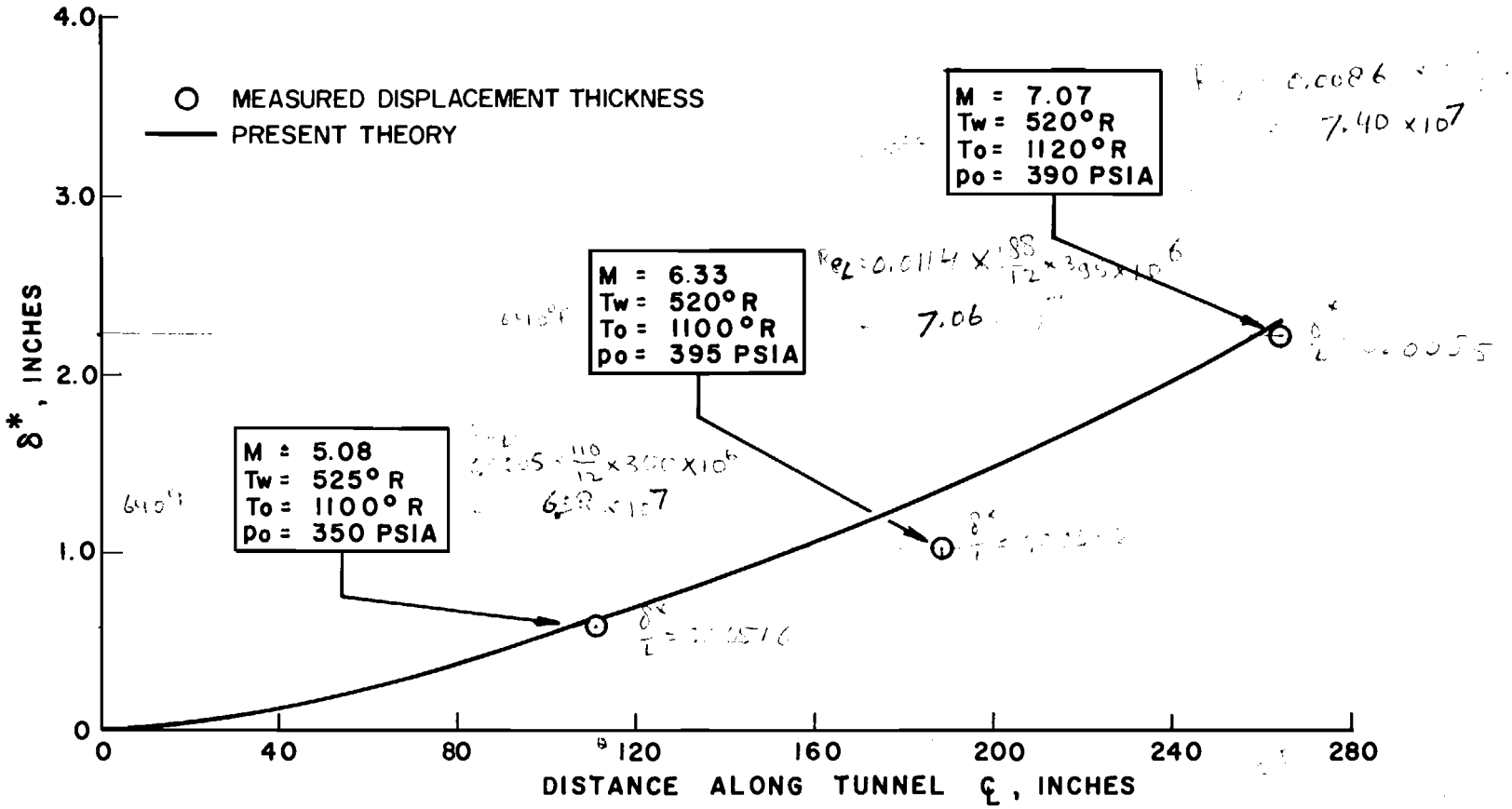

Fig. 6 Comparison of Calculated Boundary-Layer Thickness with Values Measured in a Mach 7, 50-inch-Diameter Conical Nozzle

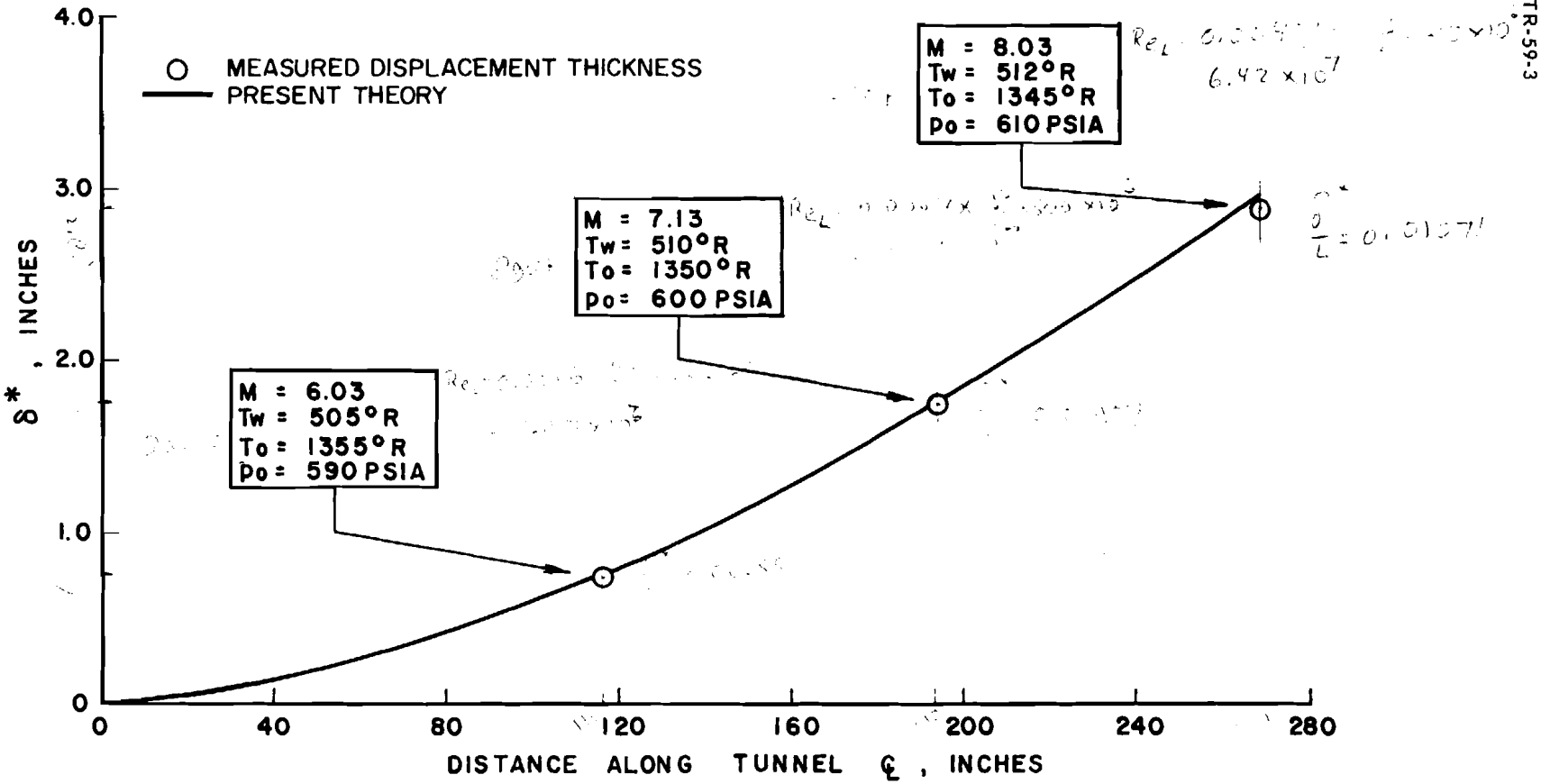

Fig. 7 Comparison of Calculated Boundary-Layer Thickness with Values Measured in a Mach 8, 50-inch-Diameter Conical Nozzle

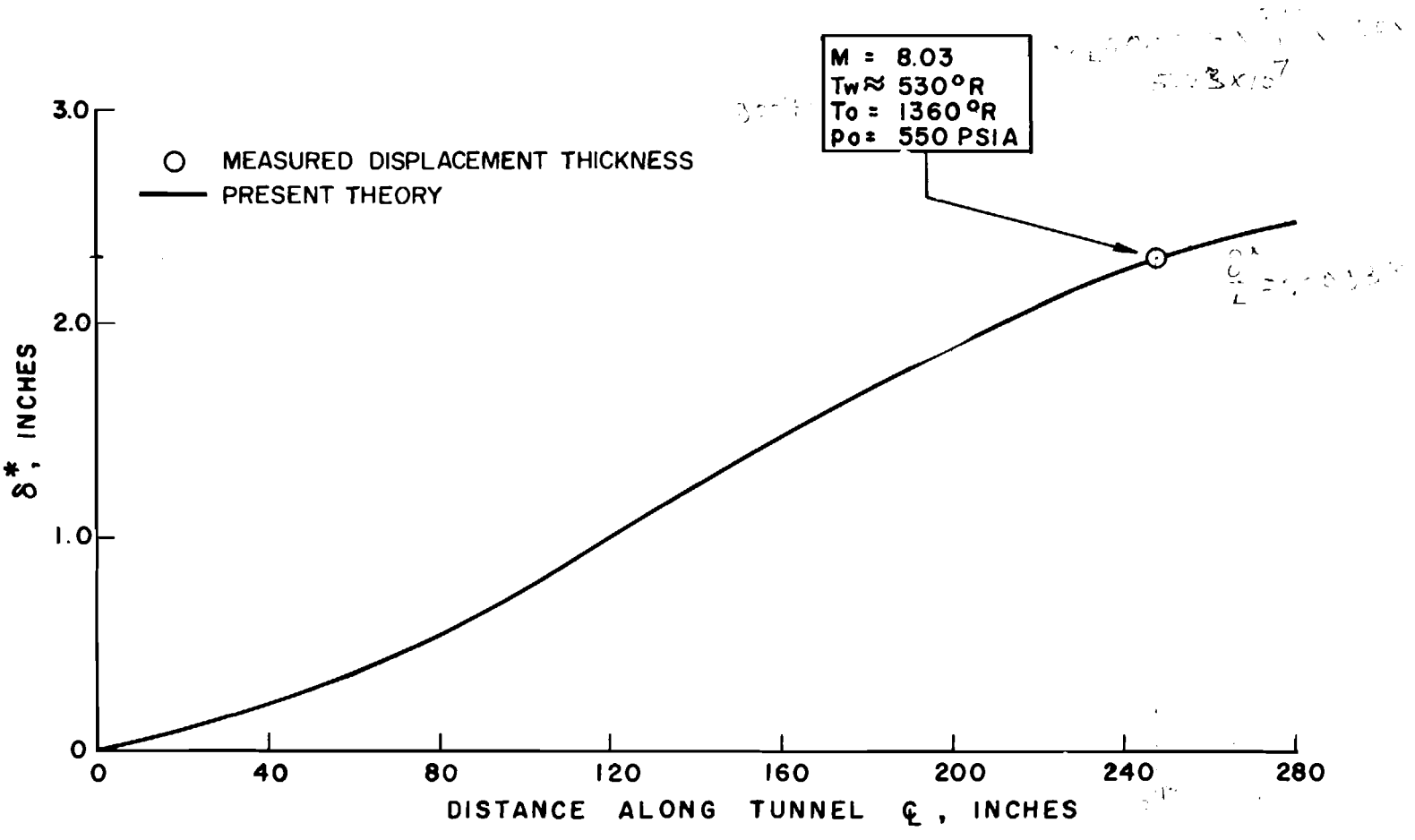

Fig. 8 Comparison of Calculated Boundary-Layer Thickness with Value Measured in a Mach 8, 50-inch-Diameter Contoured Nozzle

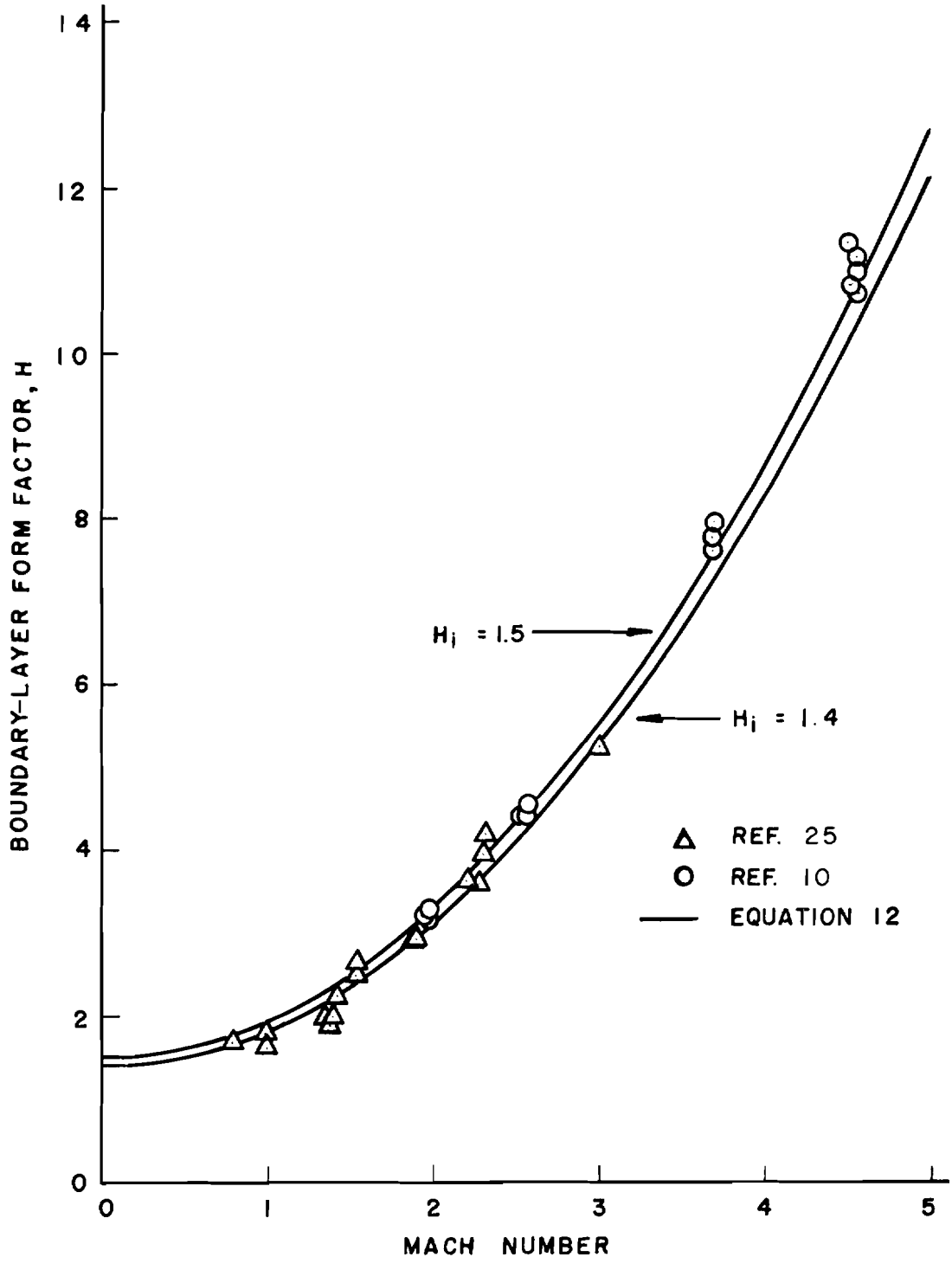

Fig. 9 Correlation of Calculated Values of H with Experimental Values

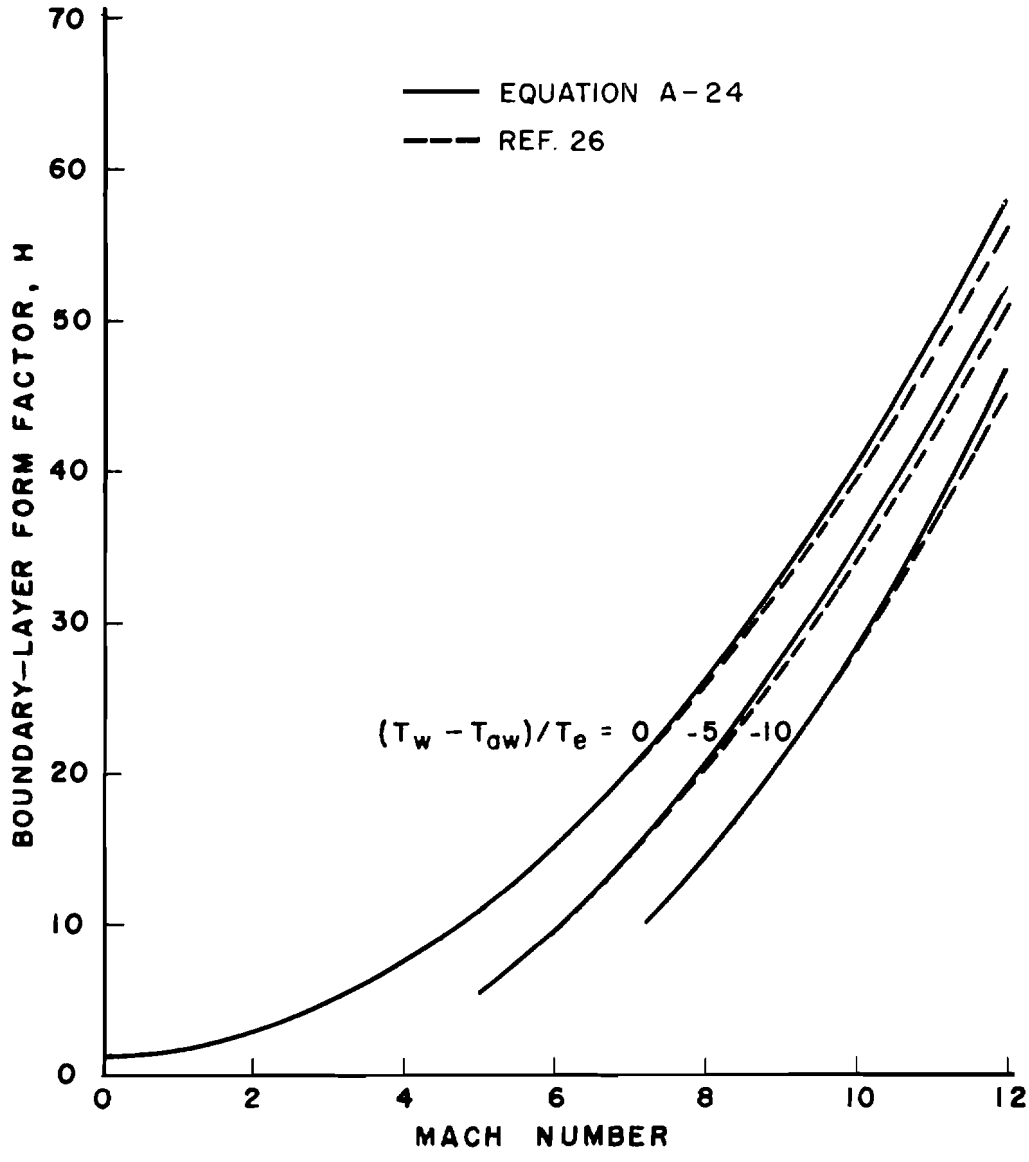

Fig. 10 Comparison of Values of H Calculated from Eq. (A-24) with Those from Ref. 26 for $H_i = 11/9$

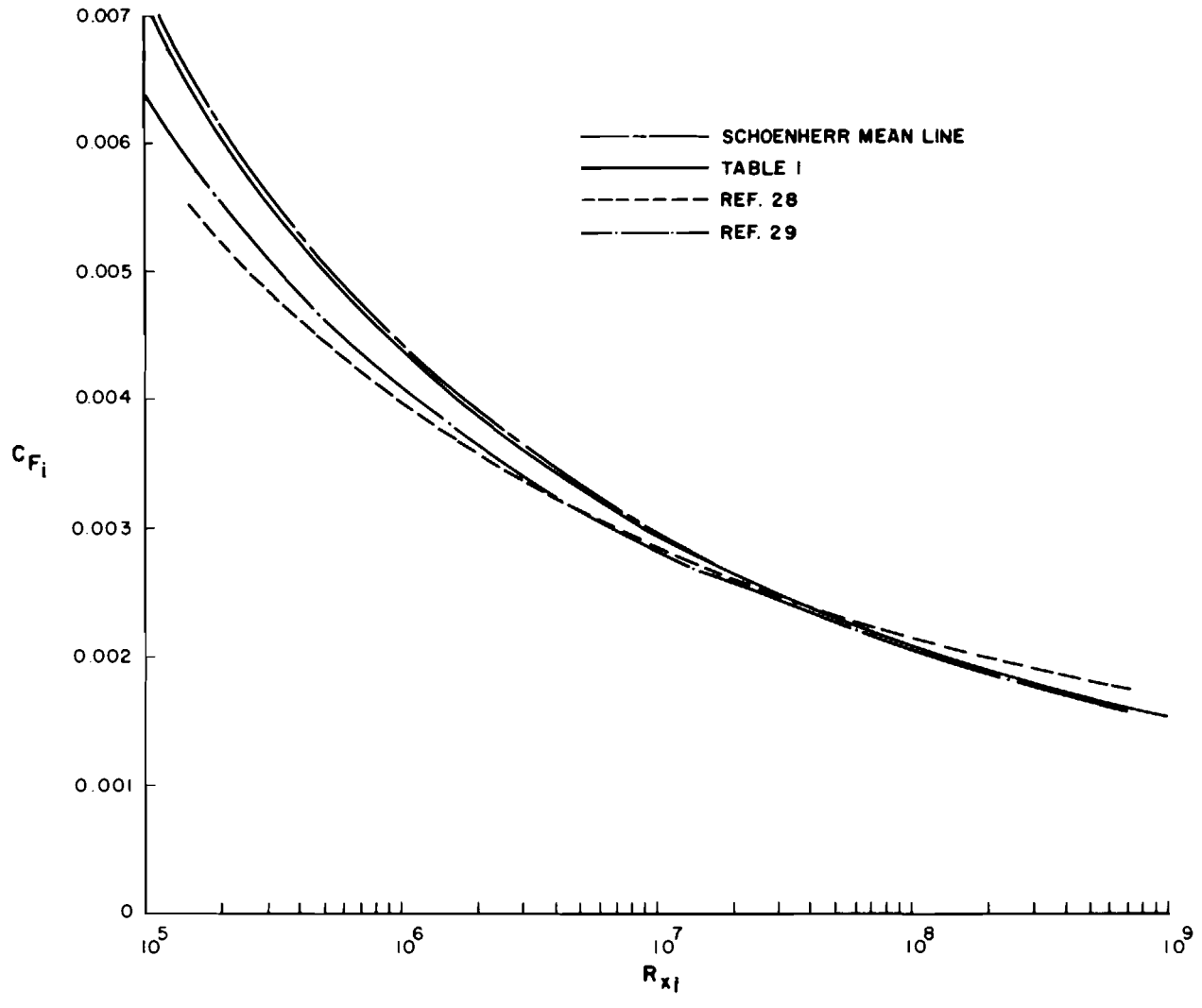

Fig. 11 Comparison of Various Equations for Incompressible Mean Skin-Friction Coefficient

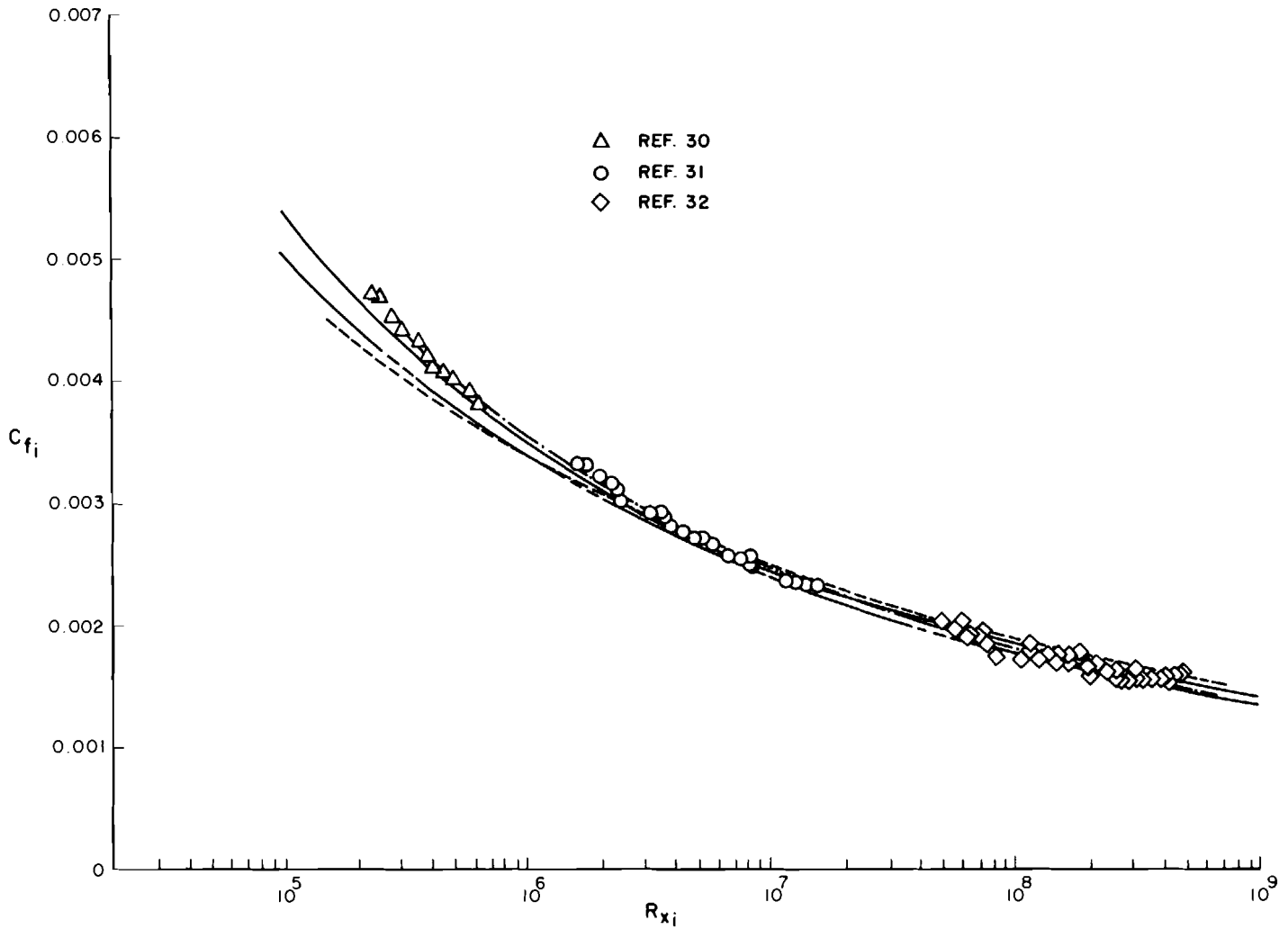

Fig. 12 Comparison of Various Equations for Incompressible Local Skin-Friction Coefficient

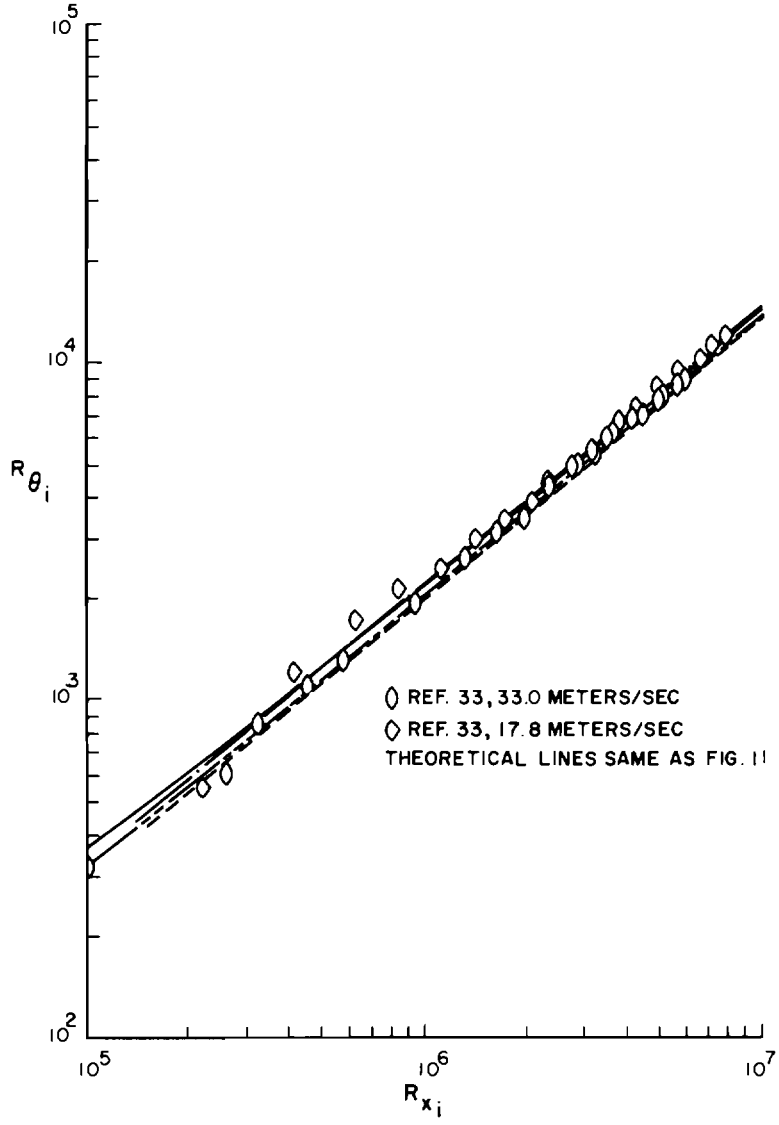

Fig. 13 Comparison of Various Equations Relating R_{θ_i} with R_{x_i}

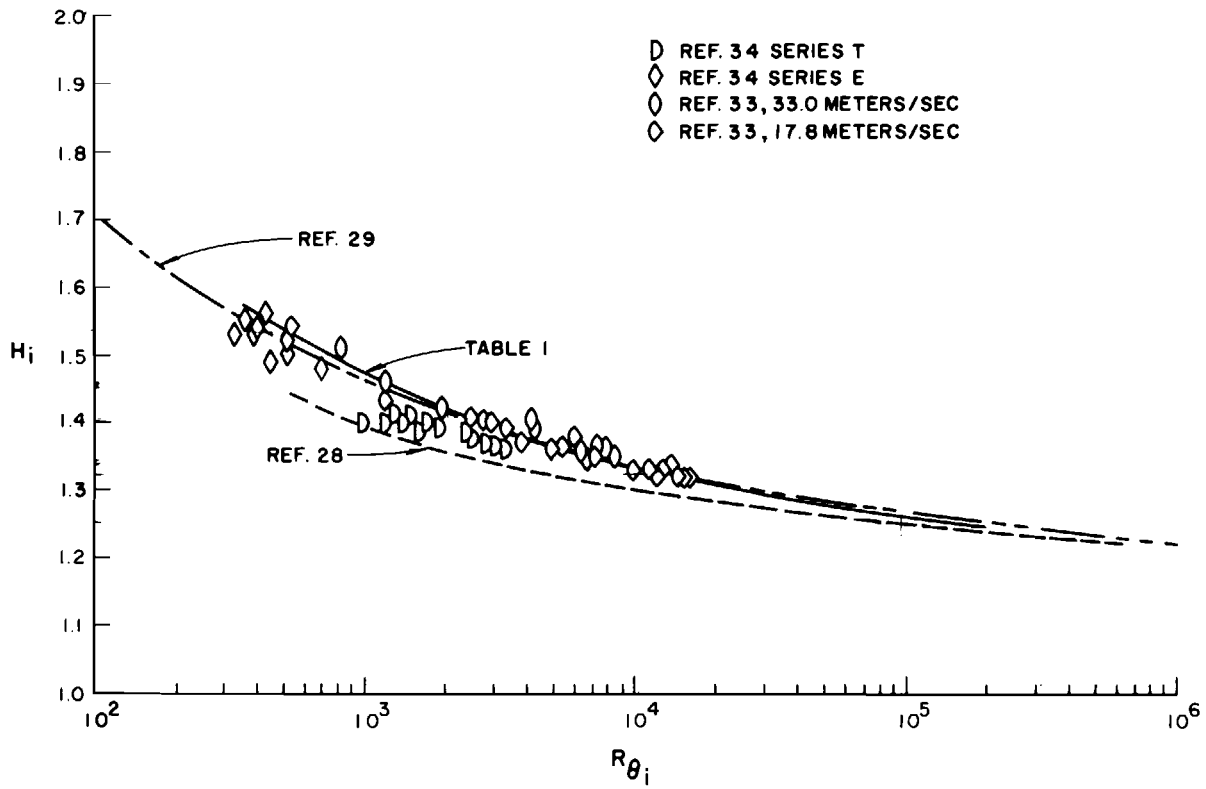

Fig. 14 Comparison of Various Equations Relating H_i with R_{θ_i}

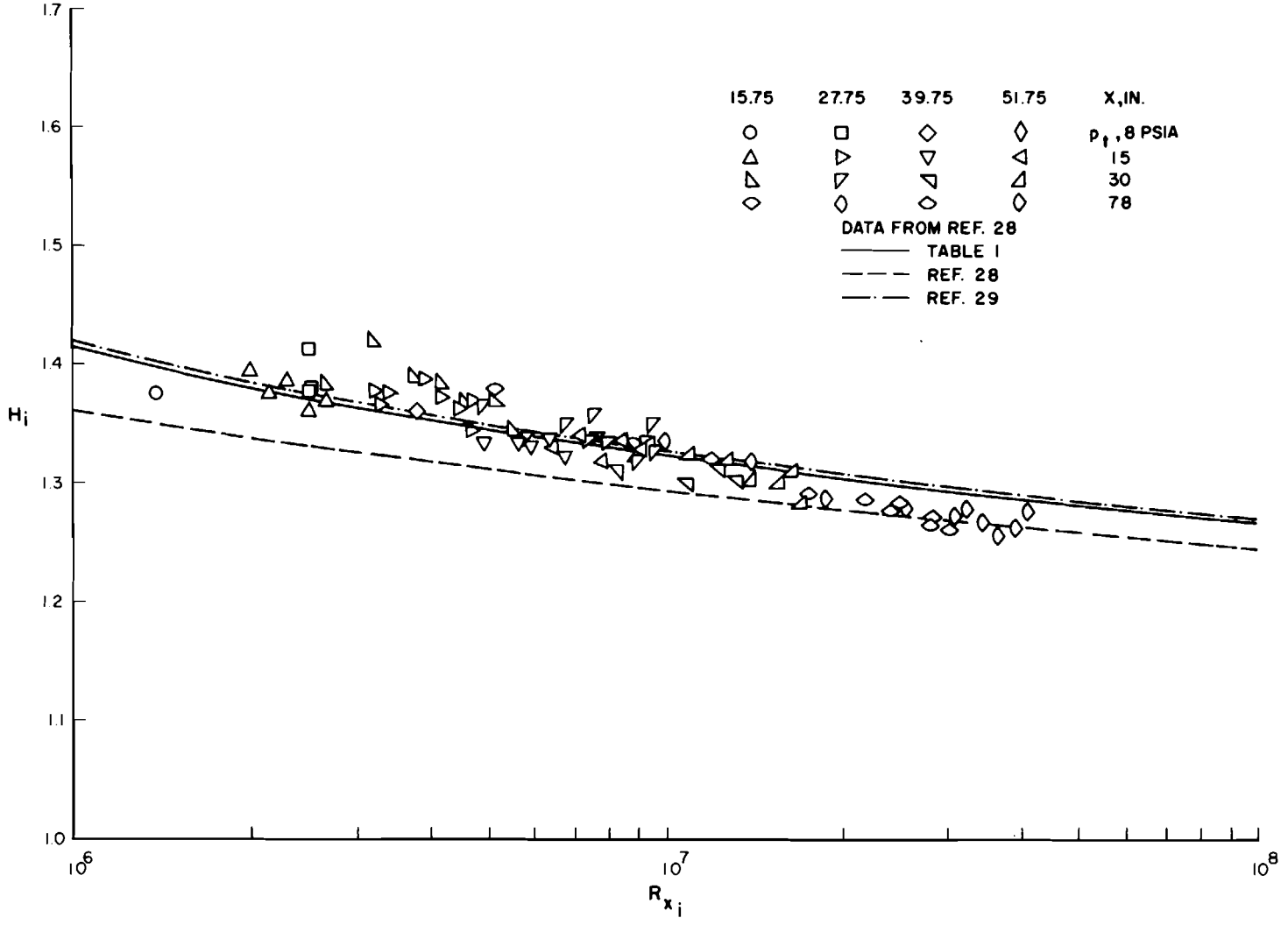

Fig. 15 Comparison of Various Equations Relating H_i with R_{x_i}